Running title: Study of post-transcriptional regulation in pigs

Modeling microRNA-driven post-transcriptional regulation by using exon-intron split analysis (EISA) in pigs

Emilio Mármol-Sánchez[1*], Susanna Cirera[2], Laura M. Zingaretti[3], Mette Juul Jacobsen[2], Yuliaxis Ramayo-Caldas[4], Claus B. Jørgensen[2], Merete Fredholm[2], Tainã Figueiredo Cardoso[1†], Raquel Quintanilla[4], Marcel Amills[1,5]

[1]Centre for Research in Agricultural Genomics (CRAG), CSIC-IRTA-UAB-UB, Universitat Autònoma de Barcelona, 08193 Bellaterra, Spain. [2]Department of Veterinary and Animal Sciences, Faculty of Health and Medical Sciences, University of Copenhagen, 1871 Frederiksberg C, Denmark. [3]Universidad Nacional de Villa María, Villa María, Córdoba, Argentina. [4]Animal Breeding and Genetics Program, Institute for Research and Technology in Food and Agriculture (IRTA), Torre Marimon, 08140 Caldes de Montbui, Barcelona, Spain. [5]Departament de Ciència Animal i dels Aliments, Universitat Autònoma de Barcelona, 08193 Bellaterra, Barcelona, Spain.

*Emilio Mármol-Sánchez current address: Science for Life Laboratory, Department of Molecular Biosciences, The Wenner-Gren Institute. Stockholm University, Stockholm, Sweden.

[†]Tainã Figueiredo Cardoso current address: Embrapa Pecuária Sudeste, Empresa Brasileira de Pesquisa Agropecuária (EMBRAPA), 13560-970, São Carlos, SP, Brazil.

Corresponding author: Emilio Mármol-Sánchez. Science for Life Laboratory, Department of Molecular Biosciences, The Wenner-Gren Institute. Stockholm University, Stockholm, Sweden. Email: emilio.marmol.sanchez@gmail.com

Emilio Mármol-Sánchez: emilio.marmol.sanchez@gmail.com

Susanna Cirera: scs@sund.ku.dk

Laura M. Zingaretti: m.lau.zingaretti@gmail.com

Mette Juul Jacobsen: pmn418@alumni.ku.dk

Yuliaxis Ramayo-Caldas: yuliaxis@gmail.com; yuliaxis.ramayo@irta.cat

Claus B. Jørgensen: clausbj@sund.ku.dk

Merete Fredholm: mf@sund.ku.dk

Tainã Figueiredo Cardoso: tainafcardoso@gmail.com

Raquel Quintanilla: raquel.quintanilla@irta.cat

Marcel Amills: Marcel.Amills@uab.cat

Abstract

The contribution of microRNAs (miRNAs) to mRNA regulation has often been explored by selecting specific downregulated genes and determining whether they harbor binding sites for miRNAs. One essential flaw of this approach is that it does not discriminate whether mRNA downregulation takes place at the transcriptional or post-transcriptional level. In the current work, we aimed to overcome this limitation by performing an exon-intron split analysis (EISA) on skeletal muscle and adipose tissue RNA-seq data from two independent pig populations. Our results revealed that transcriptional (Tc) signals were more prevalent than post-transcriptional (PTc) signals. We also observed important discrepancies between differentially expressed genes and those detected with EISA, demonstrating that the combination of both approaches yields a more comprehensive view about the molecular processes under study. Moreover, a total of 43 and 25 mRNA genes showed high PTc signals in adipose and skeletal muscle tissues, respectively. From these, 25 and 21 genes were predicted as mRNA targets of upregulated miRNAs in adipose and skeletal muscle tissues, respectively. Enrichment analyses of the number of targeted genes by upregulated miRNAs revealed relevant results only for the skeletal muscle dataset, suggesting that in this diet challenged experimental system the contribution of miRNAs to mRNA repression is more prominent. Finally, we identified several genes that may play relevant roles in the energy homeostasis of the pig skeletal muscle (e.g. *DKK2* and *PDK4*) and adipose (e.g. *SESN3* and *ESRRG*) tissues. In summary, EISA allowed us to disentangle miRNA-driven post-transcriptional regulatory signals in two distinct porcine tissues.

Keywords: Exon-intron split analysis, microRNA, pigs, energy homeostasis.

Introduction

The post-transcriptional repression of mRNA expression plays a fundamental role towards shaping fine-tuned biological responses to environmental changes (Schaefke *et al.* 2018). Such regulation can take place at multiple levels including splicing, 3′-cleavage and polyadenylation, decay or translation, and its main effectors are RNA binding proteins and non-coding RNAs (Schaefke *et al.* 2018). Of particular importance are microRNAs (miRNAs), which are primarily engaged in the post-transcriptional control of gene expression through inhibition of translation and/or destabilization of target mRNAs by poly(A) shortening and subsequent degradation (Bartel 2018).

A high number of differential expression studies have been performed in pigs during the last decade (Ayuso *et al.* 2016; Benítez *et al.* 2019; Cardoso *et al.* 2017a, 2017b; Horodyska *et al.* 2018; Ovilo *et al.* 2014; Pérez-Montarelo *et al.* 2013; Pilcher *et al.* 2015; Puig-Oliveras *et al.* 2014), which have made possible to detect many genes that are downregulated in response to certain stimuli. One of the main limitations of these studies is that the transcriptional and post-transcriptional components of gene regulation are not independently analyzed. This means that genes that are transcriptionally upregulated and post-transcriptionally downregulated, or vice versa, might not be detected as significantly differentially expressed (DE). Another disadvantage of this approach is that it does not provide insights about the causes of the observed downregulation of RNA transcripts. For instance, research studies have typically focused on specific sets of downregulated genes harboring binding sites for DE miRNAs in order to disentangle regulatory functions driven by miRNAs (Ali *et al.* 2021; Han *et al.* 2017; Iqbal *et al.* 2021; Mármol-Sánchez *et al.* 2020; Mentzel *et al.* 2015; Wei *et al.* 2018; Xie *et al.* 2019). This approach, however, is flawed by the fact that the set of downregulated genes is a mixture of loci that are repressed either at the

transcriptional or post-transcriptional levels (or both). Making such distinction is essential to understand at which level of the mRNA life-cycle regulation is taking place. Besides, relevant genes are selected after differential expression analyses and by the performance of an *ad hoc* search of predicted interactions between the 3'-UTRs of mRNAs and the seed regions of miRNAs.

A powerful approach to overcome these difficulties was developed by Gaidatzis *et al.* (Gaidatzis *et al.* 2015), who proposed that the magnitude of the post-transcriptional component can be deduced by comparing the amounts of exonic and intronic reads. Based on this assumption, these authors devised a methodology denoted *exon-intron split analysis* (EISA), which separates the transcriptional and post-transcriptional components of gene regulation. By considering that intronic reads are mainly derived from heterogeneous nuclear RNAs (unprocessed mRNAs or pre-mRNAs), they assessed the magnitude of the transcriptional regulation. Such approach is based on early reports describing the intronic expression as a proxy of nascent transcription and co-transcriptional splicing events (Ameur *et al.* 2011; Gray *et al.* 2014; Hendriks *et al.* 2014), which was later reinterpreted to infer the transcriptional fate of cells (La Manno *et al.* 2018). In this way, a gene showing similar levels of intronic reads in two different states but a strong downregulation of exonic reads after applying a certain treatment or challenge (nutrition, infection, temperature etc.), could be indicative of post-transcriptional repression (Cursons *et al.* 2018; Gaidatzis *et al.* 2015; Pillman *et al.* 2019). Previous reports have also explored the use of specific techniques to capture nascent mRNA transcripts before they are spliced (Blumberg *et al.* 2021; Core *et al.* 2008; Mahat *et al.* 2016), and these have been used to account for the transcriptional activity in a similar approach to EISA (Patel *et al.* 2020).

123 The main goal of the present study was to investigate the contribution of miRNAs to
124 post-transcriptional regulatory responses in the skeletal muscle and adipose tissue of
125 pigs by using the EISA methodology, combined with *in silico* prediction of miRNA-
126 mRNA interactions and covariation analyses. To achieve this goal, we have used two
127 different experimental systems related with porcine energy homeostasis: (1) skeletal
128 muscle samples from fasting and fed Duroc gilts, and (2) adipose tissue samples from
129 Duroc-Göttingen F_2 minipigs with divergent fatness profiles.
130
131

132 Materials and methods

133 Experimental design, sampling and processing

134 A description of the two experimental systems used to assess the importance of miRNA
135 mediated regulation of mRNA expression in pigs is provided below:
136 (i) Duroc pigs: Twenty-three gilts divided in two fasting/feeding regimes, i.e. 11 gilts
137 (*AL-T0*) slaughtered in fasting condition and 12 gilts (*AL-T2*) slaughtered immediately
138 after 7 h of having access to food (Ballester *et al.* 2018; Cardoso *et al.* 2017b; Mármol-
139 Sánchez *et al.* 2020). Immediately after slaughtering, *gluteus medius* (GM) skeletal
140 muscle samples were collected and snap-frozen at -80°C.
141 (ii) Duroc-Göttingen minipig F_2 inter-cross: Ten individuals fed *ad libitum* with
142 divergent fatness profiles for body mass index (BMI, 5 *lean* and 5 *obese*) were selected
143 from the UNIK resource population (Kogelman *et al.* 2013; Pant *et al.* 2015), as
144 described in (Jacobsen *et al.* 2019). Retroperitoneal adipose tissue was collected at
145 slaughter and mature adipocytes were subsequently isolated following Decaunes *et al.*
146 2011 with modifications reported in Jacobsen *et al.* 2019.

Further details about RNA-seq and small RNA-seq expression data generated from both experimental systems have been described in previous publications (Cardoso *et al.* 2017b; Jacobsen *et al.* 2019; Mármol-Sánchez *et al.* 2020). Sequencing reads generated in the RNA-seq and small RNA-seq datasets from both pig resources were trimmed with the Cutadapt software (Martin 2011). RNA-seq reads were mapped with the HISAT2 aligner (Kim *et al.* 2019) using default parameters. In contrast, the Bowtie Alignment v.1.2.1.1 software (Langmead *et al.* 2009) with small sequence reads specifications (*bowtie -n 0 -m 20 -k 1 --best*) was used to align small RNA-seq reads. The Sscrofa11.1 porcine reference assembly (Warr *et al.* 2020) was used to map sequences.

Exon/Intron quantification

We generated exonic and intronic-specific annotations spanning all available genes by using the gtf formatted Sscrofa.11.1 v.103 gene annotation file (Ensembl repositories: http://ftp.ensembl.org/pub/release-103/gtf/sus_scrofa/). Overlapping intronic/exonic regions, as well as singleton positions were removed (Lawrence *et al.* 2013). Each intronic region was trimmed by removing 10 nucleotides on both ends to avoid exonic reads mapping close to exon/intron junctions. We then used the *featureCounts* function included in the Rsubread package (Liao *et al.* 2019) to quantify gene expression profiles based on exon and intron expression patterns for each gene, independently. MiRNA expression profiles were estimated using the Sscrofa11.1 v.103 mature miRNA annotation with the *featureCounts* tool (Liao *et al.* 2014) in single-end mode and with default parameters.

Exon/intron split analysis (EISA).

We applied EISA to infer post-transcriptional gene regulation in our two independent porcine datasets. For this purpose, we separately estimated the exonic and intronic abundance of each annotated mRNA gene using the Sscrofa11.1 v.103 exon/intron custom annotation generated as described above. Only genes showing average expression values above 1 count-per-million in at least 50% of animals were retained for further analyses. Normalization was performed independently for exon and intron counts by multiplying each i^{th} gene expression in each j^{th} sample by the corresponding mean gene expression and dividing by the total number of quantified counts per sample (Gaidatzis *et al.* 2015). Exonic and intronic gene abundances were subsequently $\log_2$ transformed, adding a pseudo-count of 1 and averaged within each considered treatment groups (*AL-T0* and *AL-T2* for GM tissues and *lean* and *obese* for adipocyte isolates).

Only genes with exonic and intronic regions showing successfully quantified read counts were considered in our analyses. Observed differences in each i^{th} gene was expressed as the increment of exonic/intronic counts in fed (*AL-T2*) and *obese* animals with respect to fasting (*AL-T0*) and *lean* animals, respectively. In this way, the increment of intronic counts was calculated considering $\Delta Int = Int_{2i} - Int_{1i}$, whereas the increment of exonic counts (ΔEx) was also calculated considering $\Delta Ex = Ex_{2i} - Ex_{1i}$. Consequently, the transcriptional (Tc) and post-transcriptional (PTc) components were calculated. The Tc contribution to the observed counts can be explained by ΔInt, while PTc was expressed as $PTc = \Delta Ex - \Delta Int$. Both components were z-scored to represent comparable ranges between ΔEx and ΔInt estimates. We have used the intronic fraction of expressed mRNAs as a proxy of their transcriptional activity because this allows the use of RNA-seq datasets to apply EISA without the need of further experimental procedures, and it can also be applied to investigate transcriptional regulatory signals (Pillman *et al.* 2019). Correction for multiple hypothesis testing was implemented with

the Benjamini-Hochberg false discovery rate approach (Benjamini & Hochberg 1995). The statistical significance of the post-transcriptional (PTc) scores was evaluated by incorporating the intronic quantification as an interaction effect for exonic abundances (Gaidatzis *et al.* 2015), and both transcriptional (Tc) and post-transcriptional (PTc) scores were considered significant at $|FC| > 2$ and q-value < 0.05. Fasting Duroc gilts (*AL-T0*) as well as *obese* pigs from the Duroc-Göttingen line were classified as baseline controls, i.e. any given upregulation in ΔEx or ΔInt values represents and overexpression in fed (*AL-T2*) Duroc gilts or *lean* Duroc-Göttingen minipigs with respect to their fasting (*AL-T0*) and *obese* counterparts, respectively.

In order to obtain a prioritized list of genes showing relevant signals of post-transcriptional regulation, the top 5% genes with the most negative PTc scores were retrieved (irrespective of their statistical significance after multiple testing correction). We only focused on genes showing strongly reduced ΔEx values of at least 2-fold for post-transcriptional signals in both experimental systems. All implemented analyses have been summarized in **Fig. S1**. A ready-to-use modular pipeline for running EISA is publicly available at https://github.com/emarmolsanchez/EISAcompR.

Differential expression analyses

Differential expression analyses were carried out with the *edgeR* package (Robinson *et al.* 2010) by considering the exonic counts of mRNAs, as well as miRNA expression profiles of the two experimental systems under study. Expression filtered raw counts for exonic reads were normalized with the trimmed mean of M-values normalization (TMM) method (Robinson & Oshlack 2010) and the statistical significance of mean expression differences was tested with a quasi-likelihood F-test (Robinson *et al.* 2010).

Correction for multiple hypothesis testing was implemented with the Benjamini-Hochberg false discovery rate approach (Benjamini & Hochberg 1995). Messenger RNAs were considered as DE when the absolute value of the fold-change (FC) was higher than 2 ($|FC| > 2$) and q-value < 0.05. For miRNAs, $|FC| > 1.5$ and q-value < 0.05 were used instead. This more lenient fold-change threshold was motivated by the fact that miRNAs are often lowly expressed and show more stable and subtle expression changes compared to mRNAs (Guo *et al.* 2015; Mármol-Sánchez *et al.* 2020). As defined in section 2.3, fasting Duroc gilts (*AL-T0*) as well as *obese* pigs from the Duroc-Göttingen line were classified as baseline controls in differential expression analyses.

miRNA target prediction

Putative interactions between the seed regions of expressed miRNAs and the 3'-UTRs of expressed protein-coding mRNA genes were predicted on the basis of sequence identity using the Sscrofa11.1 reference assembly. The annotated 3'-UTRs longer than 30 nts from porcine mRNAs and mature miRNA sequences were retrieved from the Sscrofa11.1 v.103 annotation available at BioMart (http://www.ensembl.org/biomart) and miRBase (Kozomara *et al.* 2019) databases. Redundant seeds from mature porcine microRNAs were removed. The seedVicious v1.1 tool (Marco 2018) was used to infer miRNA-mRNA interactions. MiRNA-mRNA 8mer, 7mer-m8 and 7mer-A1 interactions were considered as the most relevant among the full set of potential ones (Bartel 2018; Friedman *et al.* 2009; Grimson *et al.* 2007).

Based on the study of Grimson *et al.* (Grimson *et al.* 2007), the *in silico*-predicted miRNA-mRNA interactions matching any of the following criteria were removed: (i) Binding sites located in 3'-UTRs at less than 15 nts close to the end of the open reading frame (and the stop codon) or less than 15 nts close to the terminal poly(A) tail (E

criterion), (ii) binding sites located in the middle of the 3'-UTR in a range comprising 45-55% of the central region of the non-coding sequence (M criterion), and (iii) binding sites that lack AU-rich elements in their immediate upstream and downstream flanking regions comprising 30 nts each (AU criterion).

Covariation patterns between miRNAs and their predicted mRNA targets were assessed by computing Spearman's correlation coefficients (ρ) with the TMM normalized and $\log_2$ transformed expression profiles of the exonic fractions of mRNA and miRNA genes. To determine the contribution of miRNAs to post-transcriptional regulation in the two experimental systems under study, only miRNA-mRNA predicted pairs comprising DE upregulated miRNAs (FC > 1.5; *q*-value < 0.05) and mRNA genes with relevant PTc scores (see post-transcriptional signal prioritization section) were taken into consideration.

miRNA target enrichment analyses

We sought to determine if the overall number of mRNA genes with high post-transcriptional signals (the ones with the top 5% negative PTc scores and reduced ΔEx values > 2-fold) were significantly enriched to be targets of at least one of the DE upregulated miRNAs (FC > 1.5; *q*-value < 0.05). That is, we predicted the overall number of targeted mRNA genes from those with high post-transcriptional signals and compared them with the number of predicted targets from the whole set of expressed mRNAs genes with available 3'-UTRs from both datasets. Enrichment analyses were carried out using the Fisher's exact test implemented in the *fisher.test* R function. Significance level was set at a nominal *P*-value < 0.05.

We also tested whether these genes were significantly enriched to be targets of at least one of the top 5% most highly expressed miRNA genes, excluding DE upregulated

miRNAs, as well as of DE downregulated miRNAs (FC < -1.5; *q*-value < 0.05). Given the relatively low statistical significance of DE miRNAs observed in the UNIK Duroc-Göttingen minipigs (l*ean* vs *obese*), we considered miRNAs that were significantly (FC < -1.5; *q*-value < 0.05) and suggestively (FC > 1.5 and *P*-value < 0.01) upregulated as potential mRNA regulators.

Gene covariation network and covariation enrichment score

We computed pairwise correlation coefficients among the whole set of mRNA genes with *q*-value < 0.05 after differential expression analyses in the *AL-T0* vs *AL-T2* (N = 454 genes) and *lean* vs *obese* (N = 299 genes). These correlations were compared with those corresponding to the set of genes with relevant post-transcriptional signals and putatively targeted by DE upregulated miRNAs. Normalized exonic and intronic estimates in the $\log_2$ scale obtained from EISA analyses were used to compute Spearman's correlation coefficients (ρ) for each potential pair of mRNA genes plus those showing post-transcriptional signals. Self-correlation pairs were excluded. Significant correlations were identified with the Partial Correlation with Information Theory (PCIT) network inference algorithm (Reverter & Chan 2008) implemented in the *pcit* R package (Watson-Haigh *et al.* 2010). Non-significant covarying pairs were set to zero, while a value of 1 was assigned to the significant ones with both positive or negative coefficients $|\rho| > 0.6$.

The potential contribution of miRNAs to the observed covariation patterns was assessed by calculating a covariation enrichment score (CES) following Tarbier *et al.* 2020 (Tarbier *et al.* 2020). Significant differences among the set of exonic, intronic and control CES values were tested with a non-parametric approach using a Mann-Whitney

296 U non-parametric test (Mann & Whitney 1947). Further details can be found in
297 **Supplementary Methods**.
298
299 **Estimating the expression levels of miRNAs and several of their predicted mRNA**
300 **targets by qPCR**
301 The same total RNA extracted from adipocytes of *lean* and *obese* minipigs (according
302 to BMI profiles, **Table S1**), and used in the RNA-seq experiment was subsequently
303 employed for cDNA synthesis and qPCR verification. We chose the adipose tissue as
304 target for qPCR analyses because the available RNA had a better quality than in skeletal
305 muscle samples. Five mRNAs (*LEP*, *OSBPL10*, *PRSS23*, *RNF157* and *SERPINE2*)
306 among those with the top 5% post-transcriptional signal were selected for qPCR
307 profiling. Two reference genes (*TBP* and *ACTB*, as defined by Nygard *et al.* 2007, were
308 used for normalization. Accordingly, three of the most significantly upregulated
309 miRNAs were selected for qPCR profiling (ssc-miR-92b-3p, ssc-miR-148a-3p and ssc-
310 miR-214-3p), plus two highly expressed non-DE miRNAs for normalization (ssc-let-7a
311 and ssc-miR-23a-3p) from the *lean* vs *obese* small RNA-seq dataset. Further details
312 about qPCR experimental procedures are available in **Supplementary Methods**. All
313 primers for mRNA and miRNA expression profiling are available at **Table S2**. Raw Cq
314 values for each assay are available at **Table S3**.
315
316
317 # Results
318 **The analysis of post-transcriptional regulation in muscle samples from fasting and**
319 **fed Duroc gilts**
320 *Differential expression and EISA analyses*

After the processing, mapping and quantification of mRNA and miRNA expression levels in GM skeletal muscle samples from Duroc gilts, an average of 45.2 million reads per sample (~93%) were successfully mapped to 31,908 genes annotated in the Sscrofa11.1 v.103 assembly (including protein coding and non-coding genes). Besides, an average of 2.2 million reads per sample (~42%) mapped to 370 annotated porcine miRNA genes.

A total of 30,322 (based on exonic reads) and 22,769 (based on intronic reads) genes were successfully quantified after splitting the reference Sscrofa11.1 v.103 assembly between exonic and intronic features. The exonic fraction displayed an average of 1,923.94 estimated counts per gene, whereas the intronic fraction showed an average of 83.02 counts per gene. In other words, exonic counts were ~23 fold more abundant than those corresponding to intronic regions.

Differential expression analyses based on exonic fractions identified 454 mRNA genes with q-value < 0.05 (**Table S4**). Among these, only genes with |FC| > 2 were retained, making a total of 52 upregulated and 80 downregulated genes in the *AL-T0* vs *AL-T2* comparison (**Table S4** and **Fig. S2a**). Besides, differential expression analyses on small RNA-seq data revealed 16 DE miRNAs, of which 8 were upregulated in *AL-T2* pigs, representing 6 unique miRNA seeds (**Table S5**). These non-redundant seeds of miRNAs significantly upregulated in fed animals (ssc-miR-148a-3p, ssc-miR-7-5p, ssc-miR-30-3p, ssc-miR-151-3p, ssc-miR-374a-3p and ssc-miR-421-5p) were selected as potential post-transcriptional regulators of GM muscle mRNA expression in response to nutrient supply.

On the other hand, EISA made possible to detect 133 genes with significant PTc scores (|FC| > 2; q-value < 0.05, **Table S6**), of which three had at least 2-fold reduced ΔEx fractions and two out from these three had negative PTc scores among the top 5% with

most negative ones (**Table 1** and **Table S6**). Among these 133 genes, only seven were also DE (5.26%, **Tables S4** and **S6**). When we analyzed the results provided by EISA regarding the transcriptional component (Tc), 344 genes displayed significant Tc scores (|FC| > 2; *q*-value < 0.05, **Table S6**). Among these 344 genes, 71 were also DE (20.63%, **Tables S4** and **S6**). Besides, 90 out of the 344 genes (26.16%) also showed significant PTc scores (**Table S6**), but none of them were among the mRNA genes displaying the top 5% negative PTc scores with at least 2-fold ΔEx reduction (N = 26, **Table 1**).

To assess the contribution of miRNAs to the post-transcriptional regulation of mRNAs, protein-encoding genes displaying the top 5% negative PTc scores with at least 2-fold ΔEx reduction (N = 26, **Table 1** and **Fig. S2b**) were selected as putative miRNA-targets. One of them (ENSSSCG00000049158) did not have a properly annotated 3´-UTR so it was excluded from further analyses. Among this set of genes with high post-transcriptional signals (N = 25), 19 of them (76%) appeared as significantly downregulated (FC < -2; *q*-value < 0.05, **Table 1** and **Table S4**).

Context-based pruning of predicted miRNA-mRNA interactions removes spurious unreliable target events

As a first step to determine if mRNA genes with highly negative PTc scores and showing a marked reduction in exonic fractions were repressed by the 6 miRNAs upregulated in the muscle tissue of *AL-T2* gilts (**Table S5**), we investigated the accuracy and reliability of *in silico* predictions of miRNA binding sites in the 3'-UTRs of these mRNAs (**Table S7**). We evaluated the enrichment in the number of genes with binding sites for at least one of the 6 miRNAs under consideration (ssc-miR-148a-3p, ssc-miR-7-5p, ssc-miR-30-3p, ssc-miR-151-3p, ssc-miR-374a-3p and ssc-miR-421-5p) over a

371 random background of expressed genes with no context-based removal of predicted
372 binding sites (see Methods). As depicted in **Figs. S3A** and **S3B**, introducing additional
373 context-based filtering criteria for removing spurious unreliable binding site predictions
374 resulted in an overall increased enrichment of genes predicted to be targeted by
375 miRNAs within the list of the top 1% (N = 12 genes, **Fig. S3a**) and 5% (N = 25 genes,
376 **Fig. S3b**) genes with negative PTc scores and displaying at least 2-fold ΔEx reduction.
377 This significant enrichment was more evident when using the AU criterion, as shown in
378 **Fig. S3a**. However, we also detected a slight increment when adding the other two
379 context-based removal criteria (M and E). These findings were more prominent when
380 taking into consideration the list of the top 1% genes (**Fig. S3a**) compared with that of
381 the top 5% genes (**Fig. S3b**). Nevertheless, an increased enrichment for targeted
382 mRNAs by DE upregulated miRNAs was detectable for all combined filtering criteria,
383 especially for 7mer-A1 binding sites, and probably at the expense of the scarcer and
384 more efficient 8mer binding sites.
385
386 *Genes with relevant post-transcriptional signals detected with EISA are predicted*
387 *targets of upregulated miRNAs*
388 Target prediction and context-based pruning of miRNA-mRNA interactions for mRNA
389 genes displaying the top 5% negative PTc scores and at least 2-fold reduction in the
390 ΔEx exonic fraction (N = 25 after excluding ENSSSCG00000049158; **Table 1**, **Fig. 1a**)
391 made possible to detect 11 8mer, 21 7mer-m8 and 22 7mer-A1 miRNA binding sites,
392 corresponding to the six non-redundant seeds of DE miRNAs upregulated in *AL-T2* gilts
393 (**Table S5**), in 21 out of the 25 analyzed mRNAs (84%, **Table S7**). Moreover, 15 out of
394 these 21 genes (71.43%) were also DE (**Table 1**).

This set of 21 mRNA genes with putative post-transcriptional repression mediated by miRNAs showed a significant enrichment in 8mer, 7mer-m8 and 7mer-A1 sites for the 6 DE miRNAs upregulated in *AL-T2* fed gilts, and this was especially relevant when combining these three types of binding sites (**Fig. 1b**). The miRNAs with the highest number of significant miRNA-mRNA correlation interactions were ssc-miR-30a-3p and ssc-miR-421-5p, which showed nine and eight significant miRNA-mRNA interactions, followed by ssc-miR-148-3p with four significant interactions with mRNA genes displaying significant post-transcriptional signals (**Table S7**).

We also evaluated the enrichment of the mRNA genes within the list of the top 5% negative PTc scores and at least 2-fold ΔEx reduction (N = 25, **Table 1**) to be targeted by the following sets of miRNAs: (i) Non-redundant miRNA seeds downregulated in *AL-T2* fed gilts (ssc-miR-1285, ssc-miR-758, ssc-miR-339, sc-miR-22-3p, ssc-miR-296-5p, ssc-miR-129a-3p, ssc-miR-181c and ssc-miR-19b, **Table S5**), (ii) the top 5% most expressed miRNAs, excluding those being also upregulated (ssc-miR-1, ssc-miR-133a-3p, ssc-miR-26a, ssc-miR-10b, ssc-miR-378, ssc-miR-99a-5p, ssc-miR-27b-3p, ssc-miR-30d, ssc-miR-486 and ssc-let-7f-5p), and (iii), iterative (N = 100) random sets of 10 expressed miRNAs, irrespective of their DE and abundance status, as a control test. None of these additional analyses recovered a significant enrichment for any type of the three considered miRNA target subtypes (**Fig. 1b**).

The mRNA with the highest and most significant PTc score was the Dickkopf WNT Signaling Pathway Inhibitor 2 (*DKK2*), so this gene was a strong candidate to be repressed by miRNAs (**Table 1**). Indeed, *DKK2* was the only gene harboring two miRNA 8mer binding sites (**Table S7**). Interestingly, this locus was not DE according to differential expression analyses (**Table 1** and **Table S4**). The discordance between EISA and differential expression results can be fully appreciated by comparing **Fig. 1a**

(genes with high post-transcriptional repression after EISA) and **Fig. 1c** (differential expression analysis), where only 19 out of the 26 initial mRNA genes highlighted by EISA appeared as significantly downregulated in the differential expression analysis (**Table 1**). Although several of the mRNA genes shown in **Table 1** were highly downregulated (**Table S4**), e.g. pyruvate dehydrogenase kinase 4 (*PDK4*), solute carrier organic anion transporter 4A1 (*SLCO4A1*), neuron navigator 2 (*NAV2*) or actin binding Rho activating protein (*ABRA*), the remaining ones were mildly to slightly downregulated or not DE.

Genes showing post-transcriptional regulatory signals predominantly covary at the exonic level

To further elucidate whether mRNA genes displaying the top 5% PTc scores are putatively targeted by common miRNAs according to *in silico* predictions (N = 21), we evaluated the covariation patterns among them and with the whole set of 454 mRNA genes (q-value < 0.05) in the *AL-T0* vs *AL-T2* comparison.

By calculating CES values (see Methods) for the 21 genes putatively targeted by DE upregulated miRNAs, we obtained an estimation of the fold change in their observed covariation with respect to the remaining mRNAs under consideration (N = 435, which results from removing the 19 DE downregulated mRNAs as shown in **Table 1** from the initial list of 454 genes with q-value < 0.05, **Table S4**). CEs values were measured for both exonic and intronic fractions. Our analyses revealed that 19 out of 21 genes showed an average increased covariation of approximately 2-fold in their exonic fractions when compared to their intronic fractions (**Table S8**, **Fig. 1d**), and *DKK2* was the gene with the strongest exonic covariation change. When we iteratively analyzed the observed fold change in covariation for random sets of genes (N = 1,000), they

displayed CES ≈ 1, indicative of no covariation (**Fig. 1d**). The observed CES distributions of exonic and intronic sets were significantly different (*P*-value = 3.663E-06) after running non-parametric tests (**Fig. 1d**). This result supports that the genes displaying the top 5% PTc scores and predicted to be repressed by upregulated miRNAs are probably coregulated at the post-transcriptional level.

Studying post-transcriptional signals in adipose tissue using a Duroc-Göttingen minipig population

After pre-processing and filtering of sequenced reads from adipocytes samples, we were able to retrieve ~98.1 and ~0.87 million mRNA and small RNA reads per sample, and ~96.5% and ~73.4% of these reads mapped to annotated porcine mRNA and miRNA genes, respectively. Differential expression analyses revealed a total of 299 mRNAs with *q*-value < 0.05, of which 52 were downregulated and 95 were upregulated (FC > |2|; *q*-value < 0.05) DE genes, respectively (**Table S9**). Regarding miRNAs, only one gene (ssc-miR-92b-3p) was significantly upregulated in *lean* pigs, while seven additional miRNAs showed suggestive differential expression (*P*-value < 0.01), of which three were downregulated, and four were upregulated (ssc-miR-148a-3p, ssc-miR-204, ssc-miR-92a and ssc-miR-214-3p). It is worth to mention that ssc-miR-92a shares the same seed sequence as ssc-miR-92b-3p (**Table S10**).

After running EISA on the mRNA expression profiles for exonic and intronic fractions, only the sestrin 3 (*SESN3*) gene showed a significant PTc score. This gene was the one with the second highest negative PTc score (**Table 2** and **Table S11**). Similar to results obtained for *DKK2* gene in *AL-T2* gilts, the *SESN3* gene was the only one showing post-transcriptional downregulation with no additional transcriptional repression detected. Moreover, *SESN3* was also detected as the most significantly downregulated gene

(**Table S9**). Regarding Tc scores, a total of 195 genes showed significant transcriptional signals (|FC| > 2; *q*-value < 0.05, **Table S11**), and 48 of them were also DE (24.61%, **Tables S9** and **S11**). Moreover, three of them (*ARHGAP27, CDH1* and *LEP*) were found among those with the top 5% post-transcriptional signals (**Table 2** and **Table S11**). The whole set of mRNA genes identified with EISA is available at **Table S11**.

A total of 44 downregulated mRNAs in *lean* pigs displayed the top 5% PTc scores with reduced ΔEx of at least 2-fold (**Table 2**, **Fig. 2a**). One of them (ENSSSCG00000016928) did not have a properly annotated 3´-UTR and was therefore excluded from further analyses. Among the remaining 43 genes with high post-transcriptional signals, only 13 of them (30.23%) appeared as significantly downregulated (FC < -2; *q*-value < 0.05) in the differential expression analysis considering exonic fractions (**Table S9** and **Table 2**).

From the set of 43 downregulated mRNAs analyzed for miRNA binding sites, 25 of them (58.14%) were classified as putative targets of the set of miRNAs upregulated in *lean* pigs (N = 4, ssc-miR-92b-3p, ssc-miR-148a-3p, ssc-miR-204 and ssc-miR-214-3p; **Table S10**). Target prediction and context-based pruning of miRNA-mRNA interactions for these 25 mRNA genes made possible to detect eight 8mer, 21 7mer-m8 and 24 7mer-A1 miRNA binding sites (**Table S12**) corresponding to the non-redundant seeds of selected upregulated miRNAs (N = 4) in *lean* minipigs (**Table S10**). The *SESN3* gene showed the highest number of predicted putative miRNA target sites in its 3´-UTR (**Table S12**).

Enrichment analyses for the set of putative miRNA target genes with the top 5% negative PTc scores and at least 2-fold ΔEx reduction (N = 25, **Table 2**) revealed no significant enrichment for the three types of miRNA target sites corresponding to the 4 upregulated miRNAs under investigation (ssc-miR-92b-3p, ssc-miR-148a-3p, ssc-miR-

204 and ssc-miR-214-3p), although a slight increase of statistical significance was obtained when considering 8mer + 7mer-m8 binding sites and all three types together (**Fig. 2b**). Among this set of 25 genes, only seven of them (28%) appeared as DE downregulated genes (FC < -2; *q*-value < 0.05) in the differential expression analysis considering their exonic fractions (**Table S9** and **Table 2**, **Fig. 2c**).

In agreement with results obtained for the skeletal muscle expression dataset, the exonic fraction of the mRNA genes putatively targeted by upregulated miRNAs in *lean* pigs showed approximately 2-fold significantly increased covariation (*P*-value = 2.703E-02) with regard to their intronic fraction (**Fig. 2d**). Besides, 18 out of these 25 mRNA genes showed an overall increased covariation in their exonic fractions compared with their intronic fractions, expressed as the increment in their CES values (ΔCES = exonic CES – intronic CES, **Table S13**).

Quantitative PCR analyses were performed to assess whether mRNAs among those highlighted by post-transcriptional signal prioritization, as well as DE miRNAs upregulated in *lean* pigs, displayed patterns of expression consistent with those obtained in the RNA-seq and small RNA-seq experiments, respectively. To this end, we selected five mRNAs (i.e. *LEP*, *OSBPL10*, *PRSS23*, *RNF157* and *SERPINE2*) and three miRNAs (i.e. ssc-miR-148a-30, ssc-miR-214-3p and ssc-miR-92b-3p) for qPCR verification. All the analyzed mRNA genes showed a reduced expression in *lean* pigs compared with their *obese* counterparts (**Fig. 2e**), and the *LEP* gene was the most significantly downregulated gene (log_2FC = -1.953; *P*-value = 1.120E-03). This result was in agreement with the strong downregulation observed for *LEP* in differential expression analyses based on RNA-seq data (log_2FC = -1.957; *q*-value = 3.443E-03, **Table S9**). With regard to miRNAs, the opposite pattern of expression was observed, with all the three profiled miRNA genes being upregulated in *lean* pigs. Moreover, as

reported in **Table S10**, ssc-miR-92b-3p was the miRNA with the most significant upregulation, and also evidenced in qPCR analyses (*P*-value = 3.57E-02, **Fig. 2f**).

Discussion

Relative contributions of the Tc and PTc components of gene regulation to energy homeostasis in porcine muscle and adipose tissues

After running EISA on both muscle and adipose tissue datasets, we observed that the number of genes with significant transcriptional signals (Tc) was much higher than that of loci with significant post-transcriptional signals (PTc). Indeed, only three and one genes obtained significant PTc estimates in Duroc gilts (skeletal muscle) and intercrossed Duroc-Göttingen minipigs (adipose tissue), respectively. In contrast, several hundred genes showed significant Tc signals in both experimental systems. Such stark difference evidences that changes in gene expression induced by feeding or obesity might be mostly driven by transcriptional rather than post-transcriptional modulators. Indeed previous reports have highlighted the usefulness of EISA to predict active transcription from the analysis of intronic fractions (Pillman *et al.* 2019).

For prioritizing putative post-transcriptionally downregulated genes, we focused on those with the strongest observed downregulation based on their ΔEx values (at least 2-fold reduction) and PTc signal (top 5% negative scores). Hence, we did not consider the significance of PTc scores as a relevant criterion, as these will appear as significant only when the post-transcriptional response is not masked by the transcriptional response. This is explained by the introduction of intronic fractions as an interaction factor for modeling post-transcriptional signals in EISA (Gaidatzis *et al.* 2015). Besides, the transcriptional component is modeled directly from intronic profiles (Gaidatzis *et al.* 2015). In this way, strong and opposite transcriptional and post-transcriptional

546 responses or single post-transcriptional signals would be deemed as significant. On the
547 contrary, genes with opposite yet not sufficiently strong components and those with a
548 coordinated downregulation (even if strong) at the transcriptional and post-
549 transcriptional level will be classified as non-significant.
550
551 **Differential expression analysis and EISA highlight different sets of genes**
552 Only ~20% of genes with significant Tc and PTc components were DE according to
553 differential expression analyses. This result evidenced that differential expression
554 analysis only captures a fraction of the genes that change their mRNA expression in
555 response to a specific factor under study (feeding and obesity in this case). Thus,
556 complementing previous studies on gene regulation (Ali *et al.* 2021; Han *et al.* 2017;
557 Iqbal *et al.* 2021; Mármol-Sánchez *et al.* 2020; Mentzel *et al.* 2015; Wei *et al.* 2018;
558 Xie *et al.* 2019) with EISA might be useful to detect many additional genes that are
559 relevant for the biological processes under investigation which, otherwise, will be
560 missed.
561 Importantly, discrepancies between EISA and DE analysis were reduced when we
562 focused on genes with top 5% negative PTc scores and at least 2-fold reduction in their
563 ΔEx values: as much as 76% (skeletal muscle) and 30.23% (adipose tissue) of genes
564 identified with EISA were also detected in the DE analysis. The increase in concordance
565 between the lists of genes with strong post-transcriptional signals and significant
566 downregulation was more pronounced in the skeletal muscle experiment. This might be
567 due to the overall stronger upregulation of miRNAs observed for this dataset when
568 compared with the adipose tissue dataset. Nevertheless, not all of the genes highlighted
569 by EISA which showed putative miRNA-driven downregulation were detected as DE,
570 and among those that did, they were not always classified as the top downregulated DE

loci. Such a discrepancy is in agreement with the subtle downregulatory effects elicited by miRNAs, which are dependent on their expression level and the number of available active target sites (Bartel 2018). In this way, EISA might serve as a better approach to identify both strong and subtle post-transcriptional effects mediated by miRNAs.

Predicting the contribution of miRNAs to the post-transcriptional regulatory response in porcine muscle and adipose tissues

Since the efficacy of miRNA-based regulation on mRNA targets depends on the context of the target site within the 3'-UTR (Grimson *et al.* 2007), we have assessed the usefulness of introducing context-based filtering criteria for removing spurious *in silico*-predicted target sites for miRNAs. Using enrichment analyses, we were able to link the set of mRNAs with downregulated exonic fractions to upregulated miRNAs predicted to target them. The influence of other non-DE highly expressed miRNAs or downregulated miRNAs was ruled out by the lack of predicted targeted mRNA genes with high post-transcriptional downregulatory signals for such miRNAs. Overall, the increase of significance of enrichment analyses after applying context-based filtering for detecting miRNA target sites revealed the ability of such criteria to discriminate and remove weak or false positive target sites located within unfavored regions of mRNA 3'-UTR. However, highly efficient target sites such as the 8mer ones, although scarcer than 7mer-m8 sites, might still be functional even at unfavored positions (Denzler *et al.* 2016; Grimson *et al.* 2007; McGeary *et al.* 2019). This may partially explain the relative lack of 8mer sites found in the top post-transcriptionally regulated mRNA genes in both experimental setups.

In the skeletal muscle system, miRNA target prediction on mRNA genes with the top 5% post-transcriptional signals and at least 2-fold reduction in their exonic fractions

596 revealed that the majority of these genes (84%) showed at least one binding site for the
597 corresponding set of DE upregulated miRNAs (N = 6), thus resulting in a significant
598 enrichment of this set of genes compared with a random background. In contrast,
599 enrichment analyses did not provide significant results when analyzing the adipose
600 tissue (only around half of the highlighted genes with relevant post-transcriptional
601 signal were predicted as putative miRNA targets). This could be explained by the
602 relatively low significance of DE upregulated miRNAs found in the adipose tissue. The
603 observed difference between both systems is a clear reflection of the variable influence
604 that miRNAs might have in regulating gene expression in both tissues under different
605 experimental conditions: from a relatively strong signal when comparing the muscle
606 expression profiles of fasted vs fed Duroc guilts, to a more subtle yet still detectable
607 signal in *lean* vs *obese* Duroc-Göttingen minipigs fed *ad libitum* with a standard
608 production pig diet. Indeed, such divergent response might be explained by different
609 feeding regimes in the two experimental interventions in which the muscle tissue was
610 much more challenged. This is concurrently reflected in a more drastic gene expression
611 regulatory response.
612
613 **Covariation patterns in the expression of genes predicted to be targeted by**
614 **upregulated microRNAs**
615 We further hypothesized that genes showing relevant post-transcriptional
616 downregulatory effects might be regulated by the same set of significantly upregulated
617 miRNAs, which could induce shared covariation in their expression profiles at the
618 exonic level. In contrast, their intronic fractions would be mainly unaffected as introns
619 would have been excised prior to any given miRNA-driven downregulation. In this
620 way, an increased gene covariation might be detectable within the sets of commonly

621 targeted mRNA genes with relevant post-transcriptional signals at the exon but not at
622 the intron level, as opposed to covariation events of these set of genes with the
623 remaining DE genes. Our results revealed an increased degree of covariation between
624 genes with high post-transcriptional signals at their exonic fractions, highlighting a
625 putative coordinated downregulation by the set of significantly upregulated miRNAs.
626
627 **Several genes displaying the strongest post-transcriptional signals in porcine**
628 **muscle samples from fasting vs fed gilts are involved in glucose and lipid**
629 **metabolism**
630 From the analysis of top mRNA genes showing the strongest post-transcriptional
631 downregulatory effects in fasted vs fed gilts, several biological functions putatively
632 regulated by miRNAs were revealed. The *DKK2* gene was the one showing the highest
633 negative PTc score, and its post-transcriptional regulatory signal was also significant.
634 Moreover, this gene also showed the strongest covariation difference in its exonic
635 fraction compared with its intronic fraction. This consistent post-transcriptional
636 regulatory effect might be mediated by ssc-miR-421-5p and ssc-miR-30a-3p, two highly
637 upregulated DE miRNAs. The DKK2 protein is a member of the dickkopf family that
638 inhibits the Wnt signaling pathway through its interaction with the LDL-receptor related
639 protein 6 (LRP6). Its repression has been associated with reduced blood-glucose levels
640 and improved glucose uptake (Li *et al.* 2012), as well as with improved adipogenesis
641 (Yang & Shi 2021) and inhibition of aerobic glycolysis (Deng *et al.* 2019). These
642 results are consistent with the increased glucose usage and triggered adipogenesis in
643 muscle tissue after nutrient supply. Other additional relevant post-transcriptionally
644 downregulated mRNA genes detected by EISA were: (i) pyruvate dehydrogenase kinase
645 4 (*PDK4*), which inhibits pyruvate to acetyl-CoA conversion and hinders glucose

utilization promoting fatty acids oxidation in energy-deprived cells (Jeong *et al.* 2012; Zhang *et al.* 2014); (ii) interleukin 18 (*IL18*), that controls energy homeostasis in the muscle by inducing AMP-activated protein kinase (AMPK) (Lindegaard *et al.* 2013), a master metabolic regulator that is suppressed upon nutrient influx in cells (Jiang *et al.* 2021); (iii) nuclear receptor subfamily 4 group A member 3 (*NR4A3*), which activates both glycolytic and glycogenic factors (Zhang *et al.* 2020a), as well as β-oxidation in muscle cells (Pearen *et al.* 2013); (iv) acetylcholine receptor subunit α (*CHRNA1*) of muscle cells, linked to the inhibition of nicotine-dependent *STAT3* upregulation (Xu *et al.* 2019) that results in protection against insulin resistance in muscle (Zhang *et al.* 2020b); (v) PBX homeobox 1 (*PBX1*), a regulator of adipocyte differentiation (Monteiro *et al.* 2011); (vi) Tet methylcytosine dioxygenase 2 (*TET2*), linked to glucose-dependent AMPK phosphorylation (Wu *et al.* 2018); and (vii) BTB domain and CNC homolog (*BACH2*), associated with mTOR complex 2 (mTORC2) glucose-dependent activation (Leprivier & Rotblat 2020; Tamahara *et al.* 2017) and the repression of forkhead box protein O1 (*FOXO1*) (Itoh-Nakadai *et al.* 2017) and *PDK4* in a coordinated manner (Gopal *et al.* 2017; Mármol-Sánchez *et al.* 2020). Overall, these results would indicate that several mRNA genes with high post-transcriptional downregulatory signals might be targeted by upregulated miRNAs, which would hence result in modulating glucose uptake and energy homeostasis in myocytes in response to nutrient uptake.

On the other hand, several genes with high post-transcriptional signals were not predicted as targets of upregulated miRNAs. For instance, two circadian clock-related genes, the circadian associated repressor of transcription (*CIART*) and period 1 (*PER1*), as well as the oxysterol binding protein like 6 (*OSBPL6*) and nuclear receptor subfamily 4 group A member 1 (*NR4A1*), all showed high post-transcriptional signals. However,

none of them showed binding sites for the set of upregulated miRNAs in their 3'-UTRs, while all of them were DE (Cardoso *et al.* 2017b; Mármol-Sánchez *et al.* 2020). Although miRNAs are key post-transcriptional regulators, other alternative post-transcriptional effectors, such as long non-coding RNAs (lncRNAs) (He *et al.* 2019), circular RNAs (circRNAs) (Maass *et al.*, 2017; Memczak *et al.* 2013), RNA methylation (Zhao *et al.* 2017) or RNA binding proteins (RBPs) (Glisovic *et al.* 2008; Hentze *et al.* 2018; Velázquez-Cruz *et al.* 2021) might be at play. Besides, indirect repression via upregulated miRNAs acting over regulators of these genes, such as transcription factors, could be also a major influence on their gene expression (Patel *et al.* 2020).

Several genes displaying the strongest post-transcriptional signals in porcine adipose tissue from lean vs obese minipigs are involved in lipid metabolism and energy homeostasis

Regarding results provided by EISA using expression data from adipocytes isolated from *lean* vs *obese* Duroc-Göttingen minipigs, several of the mRNA genes that showed high post-transcriptional repression are involved in the regulation of lipid metabolism and energy homeostasis. The gene showing the highest post-transcriptional signal was the estrogen related receptor γ (*ESRRG*), which modulates oxidative metabolism and mitochondrial function in adipose tissue and inhibits adipocyte differentiation when repressed (Kubo *et al.* 2009). The second most relevant locus highlighted by EISA was *SESN3*, an activator of the mTORC2 and PI3K/AKT signaling pathway (Huang *et al.* 2018) that protects the cell from developing insulin resistance and promotes lipolysis when inhibited (Tao *et al.* 2015). This gene showed the most significant downregulation in *lean* pigs, and gathered multiple putative binding sites for all the four upregulated

696 miRNAs under study. Other genes showing significant post-transcriptional regulation
697 were the following: (i) sterile α motif domain containing 4A (*SAMD4A*), linked to the
698 inhibition of preadipocyte differentiation and leanness phenotype in knockdown
699 experiments (Chen *et al.* 2014; Liu *et al.* 2020); (ii) prostaglandin F2- receptor protein
700 (PTGFR), associated with hypertension and obesity risk (Xiao *et al.* 2015) and the
701 improvement of insulin sensitivity and glucose homeostasis when repressed (Wang *et*
702 *al.* 2018); (iii) serine protease 23 (PRSS23), that confers protective effects against
703 inflammation and reduces fasting glucose levels when inhibited (Kuo *et al.* 2020); (iv)
704 ring finger protein 157 (*RNF157*), linked to decreased fatness profiles and autophagy in
705 adipose tissue when repressed (Kosacka *et al.* 2018); (v) silencing of oxysterol binding
706 protein like 10 (*OSBPL10*) gene promotes low-density lipoprotein (LDL) synthesis and
707 inhibits lipogenesis (Perttilä *et al.* 2009); (vi) the serum levels of
708 glycosylphosphatidylinositol phospholipase 1 (GPLD1) are regulated by insulin (Bowen
709 *et al.* 2001) and linked to the development of insulin resistance and metabolic syndrome
710 (Ussar *et al.* 2012); (vii) overexpression of neutrophil cytosolic 2 (*NCF2*), the gene
711 showing the highest increase in covariation at the exonic fraction, was described in
712 obese humans (Xu *et al.* 2016); (viii) the repression of RAP1 GTPase activating protein
713 (RAP1GAP) protects against obesity and the development of insulin and glucose
714 resistance (Martinez *et al.* 2013; Yeung *et al.* 2013); and finally, (xix) leptin (*LEP*),
715 which is mainly produced in adipose tissue (Yang *et al.* 2007) and regulates appetite,
716 energy expenditure and body weight (Izquierdo *et al.* 2019; Zhou & Rui 2013). Despite
717 the overall weak influence of putative miRNA-driven downregulation found in
718 adipocytes (as evidenced by the low significance of DE upregulated miRNAs and the
719 absence of a significant target enrichment), we were able to describe a set of genes with
720 high post-transcriptional signals indicative of putative miRNA-derived repression and

721 tightly related to adipose tissue metabolism regulation. However, non-miRNA
722 transcriptional (e.g. transcription factors) and post-transcriptional (e.g. lncRNAs,
723 circRNAs, RBPs etc) modulators, together with epigenetic mechanisms, might also
724 contribute to a high proportion of the observed regulatory signals.
725
726

727 # Conclusions

728 EISA applied to study gene regulation in porcine skeletal muscle and adipose tissues
729 showed that many more genes displayed transcriptional rather than post-transcriptional
730 signals, suggesting that changes in mRNA levels are mostly driven by factors acting at
731 the transcriptional level in our study. Moreover, many genes had mixed regulatory
732 signals, either cooperative (Tc and PTc signals have the same direction) or discordant.
733 More importantly, the concordance between the sets of DE genes and those with
734 significant Tc or PTc scores was quite limited, although such difference was reduced
735 (mostly in the skeletal muscle experiment) when we prioritized the downregulated
736 genes with top post-transcriptional signals. Nevertheless, many of the genes with
737 relevant PTc signals were not among the top DE downregulated loci, thus
738 demonstrating the usefulness of complementing DE analysis with the EISA approach.
739 In the skeletal muscle, we have established a clear relationship between the set of 25
740 genes with top 5% negative PTc scores and at least 2-fold reduction in the ΔEx exonic
741 fraction and the 6 miRNAs upregulated in fed gilts and we have detected some level of
742 co-variation, suggesting that several mRNAs are co-regulated by a common set of
743 miRNAs. In contrast, in the adipose tissue such relationship was more subtle, indicating
744 that the contribution of miRNAs to mRNA repression might vary depending on the
745 tissue and experimental challenge under consideration. Finally, EISA made possible to

identify several genes related with carbohydrate and/or lipid metabolism, which may play relevant roles in the energy homeostasis of the skeletal muscle and adipose tissues. In summary, we provided compelling evidence of the usefulness of EISA to highlight relevant genes regulated at the transcriptional and/or post-transcriptional level, compared with canonical differential expression analyses. The use of EISA on commonly available RNA-seq datasets might provide novel insights into the regulatory mechanisms of the cell metabolism that previous methods were not fully able to uncover.

Ethics approval

Animal care and management procedures for Duroc gilts followed national guidelines for the Good Experimental Practices and were approved by the Ethical Committee of the Institut de Recerca i Tecnologia Agroalimentàries (IRTA). Animal care and management procedures for Duroc-Göttingen minipigs were carried out according to the Danish "Animal Maintenance Act" (Act 432 dated 9 June 2004).

Availability of data

The RNA-seq and small RNA-seq datasets from skeletal muscle tissue used in the current study are available at the Sequence Read Archive (SRA) database with BioProject codes PRJNA386796 and PRJNA595998, respectively. For the adipose tissue samples, RNA-seq and small RNA-seq datasets are available at PRJNA563583 and PRJNA759240.

Competing interests

771 The authors declare that they have no competing interests

772

773 **Funding**

774 The present research work was funded by grants AGL2013-48742-C2-1-R and
775 AGL2013-48742-C2-2-R awarded by the Spanish Ministry of Economy and
776 Competitivity. E. Mármol-Sánchez was funded with a PhD fellowship FPU15/01733
777 awarded by the Spanish Ministry of Education and Culture (MECD). YRC is recipient
778 of a Ramon y Cajal fellowship (RYC2019-027244-I) from the Spanish Ministry of
779 Science and Innovation.

780

781 **Authors' contributions**

782 The authors' responsibilities were as follows: M.A. and R.Q. designed the muscle
783 experiment. S.C., M.J.J., C.B.J. and M.F. designed the fat experiment. M.A., R.Q., S.C.,
784 M.J.J., C.B.J., M.F., T.F.C. and E.M.-S. conducted the research. S.C. performed qPCR
785 analyses. E.M.-S. analyzed the data. L.M.Z. contributed to bioinformatic analyses.
786 Y.R.-C. contributed to critical assessment. M.A. and R.Q. secured funding for the study.
787 E.M.-S., S.C. and M.A. drafted the manuscript. All authors contributed to manuscript
788 corrections, read and approved the final manuscript.

789

790 **Acknowledgements**

791 The authors would like to thank the Department of Veterinary Animal Sciences in the
792 Faculty of Health and Medical Sciences of the University of Copenhagen for providing
793 sequencing data and their facilities and resources for qPCR experiments. We also
794 acknowledge Selección Batallé S.A. for providing animal material and the support of
795 the Spanish Ministry of Economy and Competitivity for the Center of Excellence

796 Severo Ochoa 2020–2023 (CEX2019-000902-S) grant awarded to the Centre for
797 Research in Agricultural Genomics (CRAG, Bellaterra, Spain). Thanks also to the
798 CERCA Programme of the Generalitat de Catalunya for their support.

799

800

801

802 # References

803 Ali A., Murani E., Hadlich F., Liu X., Wimmers K. & Ponsuksili S. (2021) In utero fetal
804 weight in pigs is regulated by microRNAs and their target genes. *Genes* **12**, 1264.
805 Ameur A., Zaghlool A., Halvardson J., Wetterbom A., Gyllensten U., Cavelier L. *et al.*
806 (2011) Total RNA sequencing reveals nascent transcription and widespread co-
807 transcriptional splicing in the human brain. *Nature Structural & Molecular*
808 *Biology* **18**, 1435–40.
809 Ayuso M., Fernández A., Núñez Y., Benítez R., Isabel B., Fernández A.I. *et al.* (2016)
810 Developmental stage, muscle and genetic type modify muscle transcriptome in
811 pigs: Effects on gene expression and regulatory factors involved in growth and
812 metabolism. *PLoS One* **11**, e0167858.
813 Ballester M., Amills M., González-Rodríguez O., Cardoso T.F., Pascual M., González-
814 Prendes R. *et al.* (2018) Role of AMPK signaling pathway during compensatory
815 growth in pigs. *BMC Genomics* **9**, 682.
816 Bartel D.P. (2018) Metazoan microRNAs. *Cell* **173**, 20–51.
817 Benítez R., Trakooljul N., Núñez Y., Isabel B., Murani E., De Mercado E. *et al.* (2019)
818 Breed, diet, and interaction effects on adipose tissue transcriptome in Iberian and
819 duroc pigs fed different energy sources, *Genes* **10**, 589.
820 Benjamini Y. & Hochberg Y. Controlling the false discovery rate: a practical and

powerful approach to multiple testing. *Journal of the Royal Statistical Society Series B (Methodological)* **57**, 289–300.

Blumberg A., Zhao Y., Huang Y.-F., Dukler N., Rice E.J., Chivu A.G. *et al.* (2021) Characterizing RNA stability genome-wide through combined analysis of PRO-seq and RNA-seq data. *BMC Biology* **19**, 30.

Bowen R.F., Raikwar N.S., Olson L.K. & Deeg M.A. (2001) Glucose and insulin regulate glycosylphosphatidylinositol-specific phospholipase D expression in islet beta cells. Metabolism **50**, 1489–1492.

Cardoso T.F., Cánovas A., Canela-Xandri O., González-Prendes R., Amills M. & Quintanilla, R. (2017) RNA-seq based detection of differentially expressed genes in the skeletal muscle of Duroc pigs with distinct lipid profiles. *Scientific Reports* **7**, 40005.

Cardoso T.F., Quintanilla R., Tibau J., Gil M., Mármol-Sánchez E., González-Rodríguez O. *et al.* (2017) Nutrient supply affects the mRNA expression profile of the porcine skeletal muscle. *BMC Genomics* **18**, 603.

Chen Z., Holland W., Shelton J.M., Ali A., Zhan X., Won S, *et al.* (2014) Mutation of mouse *Samd4* causes leanness, myopathy, uncoupled mitochondrial respiration, and dysregulated mTORC1 signaling. *Proceedings of the National Academy of Sciences (USA)* **111**, 7367–7372.

Core L.J., Waterfall J.J. & Lis J.T. (2008) Nascent RNA sequencing reveals widespread pausing and divergent initiation at human promoters. *Science* **322**, 1845-1848.

Cursons J., Pillman K.A., Scheer K.G., Gregory P.A., Foroutan M., Hediyeh-Zadeh S. *et al.* (2018) Combinatorial targeting by microRNAs co-ordinates post-transcriptional control of EMT. *Cell Systems* **7**, 77-91.e7.

Decaunes P., Estève D., Zakaroff-Girard A., Sengenès C., Galitzky J. & Bouloumié A.

(2011) Adipose-derived stromal cells: cytokine expression and immune cell contaminants. *Methods in Molecular Biology* **702**, 151–161.

Deng F., Zhou R., Lin C., Yang S., Wang H., Li W. *et al.* (2019) Tumor-secreted dickkopf2 accelerates aerobic glycolysis and promotes angiogenesis in colorectal cancer. *Theranostics* **9**, 1001-1014.

Denzler R., McGeary S.E., Title A.C., Agarwal V., Bartel D.P. & Stoffel M. (2016) Impact of microRNA levels, target-site complementarity, and cooperativity on competing endogenous RNA-regulated gene expression. *Molecular Cell* **64**, 565-579.

Friedman R.C., Farh K.K.H., Burge C.B. & Bartel D.P. (2009) Most mammalian mRNAs are conserved targets of microRNAs. *Genome Research* **19**, 92–105.

Gaidatzis D., Burger L., Florescu M. & Stadler M.B. (2015) Analysis of intronic and exonic reads in RNA-seq data characterizes transcriptional and post-transcriptional regulation. *Nature Biotechnology* **33**, 722–729.

Glisovic T., Bachorik J.L., Yong J. & Dreyfuss G. (2008) RNA-binding proteins and post-transcriptional gene regulation. *FEBS Letters* **582**, 1977–1986.

Gopal K., Saleme B., Al Batran R., Aburasayn H., Eshreif A., Ho K.L. *et al.* (2017) FoxO1 regulates myocardial glucose oxidation rates via transcriptional control of pyruvate dehydrogenase kinase 4 expression. *American Journal of Physiology, Heart and Circulatory Physiology* **313**, H479–H490.

Gray J.M., Harmin D.A., Boswell S.A., Cloonan N., Mullen T.E., Ling J.J. *et al.* (2014) SnapShot-Seq: a method for extracting genome-wide, in vivo mRNA dynamics from a single total RNA sample. *PLoS One* **9**, e89673.

Grimson A., Farh K.K.H., Johnston W.K., Garrett-Engele P., Lim L.P. & Bartel D.P. (2007) MicroRNA targeting specificity in mammals: determinants beyond seed

pairing. *Molecular Cell* **27**, 91–105.

Guo Y., Liu J., Elfenbein S.J., Ma Y., Zhong M., Qiu C., Ding Y. *et al.* (2015) Characterization of the mammalian miRNA turnover landscape. *Nucleic Acids Research* **43**, 2326–2341.

Han H., Gu S., Chu W., Sun W., Wei W., Dang X. *et al.* (2017) miR-17-5p regulates differential expression of NCOA3 in pig intramuscular and subcutaneous adipose tissue. *Lipids* **52**, 939–949.

He R.Z., Luo D.X. & Mo Y.Y. (2019) Emerging roles of lncRNAs in the post-transcriptional regulation in cancer. *Genes & Diseases* **6**, 6–15.

Hendriks G.-J., Gaidatzis D., Aeschimann F. & Großhans H. (2014) Extensive oscillatory gene expression during *C. elegans* larval development. *Molecular Cell* **53**, 380–92.

Hentze M.W., Castello A., Schwarzl T. & Preiss T. (2018) A brave new world of RNA-binding proteins. *Nature Reviews Molecular Cell Biology* **19**, 327–341.

Horodyska J., Wimmers K., Reyer H., Trakooljul N., Mullen A.M., Lawlor P.G. *et al.* (2018) RNA-seq of muscle from pigs divergent in feed efficiency and product quality identifies differences in immune response, growth, and macronutrient and connective tissue metabolism. *BMC Genomics* **19**, 791.

Huang X., Liu G., Guo J. & Su Z. (2018) The PI3K/AKT pathway in obesity and type 2 diabetes. *International Journal of Biological Sciences* **14**, 1483-1496.

Iqbal M.A., Ali A., Hadlich F., Oster M., Reyer H., Trakooljul N. *et al.* (2021) Dietary phosphorus and calcium in feed affects miRNA profiles and their mRNA targets in jejunum of two strains of laying hens. *Scientific Reports* **11**, 13534.

Itoh-Nakadai A., Matsumoto M., Kato H., Sasaki J., Uehara Y., Sato Y. *et al.* (2017) A Bach2-Cebp gene regulatory network for the commitment of multipotent

hematopoietic progenitors. *Cell Reports* **18**, 2401–2414.

Izquierdo A.G., Crujeiras A.B., Casanueva F.F. & Carreira M.C. (2019) Leptin, obesity, and leptin resistance: where are we 25 years later? *Nutrients* **11**, 2704.

Jacobsen M.J., Havgaard J.H., Anthon C., Mentzel C.M.J., Cirera S., Krogh P.M. *et al.* (2019) Epigenetic and transcriptomic characterization of pure adipocyte fractions from obese pigs identifies candidate pathways controlling metabolism. *Frontiers in Genetics* **10**, 1268.

Jeong J.Y., Jeoung N.H., Park K.-G. & Lee I.-K. Transcriptional regulation of pyruvate dehydrogenase kinase. *Diabetes & Metabolism Journal* **36**, 328–35.

Jiang P., Ren L., Zhi L., Yu Z., Lv F., Xu F. *et al.* (2021) Negative regulation of AMPK signaling by high glucose via E3 ubiquitin ligase MG53. *Molecular Cell* **81**, 629-637.e5.

Kim D., Paggi J.M., Park C., Bennett C. & Salzberg S.L. (2019) Graph-based genome alignment and genotyping with HISAT2 and HISAT-genotype. *Nature Biotechnology* **37**, 907–915.

Kogelman L.J.A., Kadarmideen H.N., Mark T., Karlskov-Mortensen P., Bruun C.S., Cirera S. *et al.* (2013) An F2 pig resource population as a model for genetic studies of obesity and obesity-related diseases in humans: Design and genetic parameters. *Frontiers in Genetics* **4**, 29.

Kosacka J., Nowicki M., Paeschke S., Baum P., Blüher M. & Klö ting N. (2018) Up-regulated autophagy: as a protective factor in adipose tissue of WOKW rats with metabolic syndrome. Diabetology & Metabolic Syndrome **10**, 13.

Kozomara A., Birgaoanu M. & Griffiths-Jones S. (2019) MiRBase: From microRNA sequences to function. *Nucleic Acids Research* **47**, D155–D162.

Kubo M., Ijichi N., Ikeda K., Horie-Inoue K., Takeda S. & Inoue S. (2009) Modulation

of adipogenesis-related gene expression by estrogen-related receptor γ during adipocytic differentiation. *Biochimica et Biophysica Acta (BBA) Gene Regulatory Mechanisms* **1789**, 71–77.

Kuo C.-S., Chen J.-S., Lin L.-Y., Schmid-Schönbein G.W., Chien S., Huang P.-H. *et al.* (2020) Inhibition of serine protease activity protects against high fat diet-induced inflammation and insulin resistance. *Scientific Reports* **10**, 1–11.

La Manno G., Soldatov R., Zeisel A., Braun E., Hochgerner H., Petukhov V. *et al.* (2018) RNA velocity of single cells. *Nature* **560**, 494–498.

Langmead B., Trapnell C., Pop M. & Salzberg S.L. (2009) Ultrafast and memory-efficient alignment of short DNA sequences to the human genome. *Genome Biology* **10**, R25.

Lawrence M., Huber W., Pagès H., Aboyoun P., Carlson M., Gentleman R. *et al.* (2013) Software for computing and annotating genomic ranges. *PLoS Computational Biology* **9**, e1003118.

Leprivier G. & Rotblat B. (2020) How does mTOR sense glucose starvation? AMPK is the usual suspect. *Cell Death Discovery* **6**, 27.

Li X., Shan J., Chang W., Kim I., Bao J., Lee H.-J. *et al.* (2012) Chemical and genetic evidence for the involvement of Wnt antagonist Dickkopf2 in regulation of glucose metabolism. *Proceedings of the National Academy of Sciences (USA)* **109**, 11402–11407.

Liao Y., Smyth G.K. & Shi W. (2014) featureCounts: an efficient general purpose program for assigning sequence reads to genomic features. *Bioinformatics* **30**, 923–930.

Liao Y., Smyth G.K. & Shi W. (2019) The R package Rsubread is easier, faster, cheaper and better for alignment and quantification of RNA sequencing reads.

Nucleic Acids Research **47**, e47–e47.

Lindegaard B., Mathews V.B., Brandt C., Hojman P., Allen T.L., Estevez E. *et al.* (2013) Interleukin-18 activates skeletal muscle AMPK and reduces weight gain and insulin resistance in mice. *Diabetes* **62**, 3064–3074.

Liu Y., Liu H., Li Y., Mao R., Yang H., Zhang Y. *et al.* (2020) Circular RNA *SAMD4A* controls adipogenesis in obesity through the miR-138-5p/EZH2 axis. *Theranostics* **10**, 4705–4719.

Maass P.G., Glažar P., Memczak S., Dittmar G., Hollfinger I., Schreyer L. *et al.* (2017) A map of human circular RNAs in clinically relevant tissues. *Journal of Molecular Medicine* **95**, 1179–1189.

Mahat D.B., Kwak H., Booth G.T., Jonkers I.H., Danko C.G., Patel R.K. *et al.* (2016) Base-pair resolution genome-wide mapping of active RNA polymerases using precision nuclear run-on (PRO-seq). *Nature Protocols* **11**, 1455.

Mann H.B. & Whitney D.R. (1947) On a test of whether one of two random variables is stochastically larger than the other. *Annals of Mathematical Statistics* **18**, 50–60.

Marco A. (2018) SeedVicious: Analysis of microRNA target and near-target sites. *PLoS One* 13, e0195532.

Mármol-Sánchez E., Ramayo-Caldas Y., Quintanilla R., Cardoso T.F., González-Prendes R., Tibau J. *et al.* (2020) Co-expression network analysis predicts a key role of microRNAs in the adaptation of the porcine skeletal muscle to nutrient supply. *Journal of Animal Science & Biotechnology* **11**, 10.

Martin M. (2011) Cutadapt removes adapter sequences from high-throughput sequencing reads. *EMBnet.Journal* **17**, 10.

Martínez P., Gómez-López G., García F., Mercken E., Mitchell S., Flores J.M. *et al.* (2013) RAP1 protects from obesity through its extratelomeric role regulating

gene expression. *Cell Reports* **3**, 2059–2074.

McGeary S.E., Lin K.S., Shi C.Y., Pham T.M., Bisaria N., Kelley G.M. *et al.* (2019) The biochemical basis of microRNA targeting efficacy. *Science* **366**, eaav1741.

Memczak S., Jens M., Elefsinioti A., Torti F., Krueger J., Rybak A. *et al.* (2013) Circular RNAs are a large class of animal RNAs with regulatory potency. Nature **495**, 333–338.

Mentzel C.M.J., Anthon C., Jacobsen M.J., Karlskov-Mortensen P., Bruun C.S., Jørgensen C.B. *et al.* (2015) Gender and obesity specific microRNA expression in adipose tissue from lean and obese pigs. *PLoS One* **10**, e0131650.

Monteiro M.C., Sanyal M., Cleary M.L., Sengenès C., Bouloumié A., Dani C. *et al.* (2011) PBX1: a novel stage-specific regulator of adipocyte development. *Stem Cells* **29**, 1837–1848.

Nygard A.B., Jørgensen C.B., Cirera S. & Fredholm M. (2007) Selection of reference genes for gene expression studies in pig tissues using SYBR green qPCR. *BMC Molecular Biology* **8**, 67.

Óvilo C., Benítez R., Fernández A., Núñez Y., Ayuso M., Fernández A.I. *et al.* (2014) Longissimus dorsi transcriptome analysis of purebred and crossbred Iberian pigs differing in muscle characteristics. *BMC Genomics* **15**, 413.

Pant S.D., Karlskov-Mortensen P., Jacobsen M.J., Cirera S., Kogelman L.J.A., Bruun C.S. *et al.* (2015) Comparative analyses of QTLs influencing obesity and metabolic phenotypes in pigs and humans. *PLoS One* **10**, e0137356.

Patel R.K., West J.D., Jiang Y., Fogarty E.A. & Grimson A. (2020) Robust partitioning of microRNA targets from downstream regulatory changes. *Nucleic Acids Research* **48**, 9724–9746.

Pearen M.A., Goode J.M., Fitzsimmons R.L., Eriksson N.A., Thomas G.P., Cowin G.J.

et al. (2013) Transgenic muscle-specific Nor-1 expression regulates multiple pathways that effect adiposity, metabolism, and endurance. *Molecular Endocrinology* **27**, 1897–1917.

Pérez-Montarelo D., Fernández A., Barragán C., Noguera J.L., Folch J.M., Rodríguez M.C. *et al.* (2013) Transcriptional characterization of porcine leptin and leptin receptor genes. *PLoS One* **8**, e66398.

Perttilä J., Merikanto K., Naukkarinen J., Surakka I., Martin N.W., Tanhuanpää K. *et al.* (2009) *OSBPL10*, a novel candidate gene for high triglyceride trait in dyslipidemic Finnish subjects, regulates cellular lipid metabolism. Journal of Molecular Medicine **87**, 825–835.

Pilcher C.M., Jones C.K., Schroyen M., Severin A.J., Patience J.F., Tuggle C.K. *et al.* (2015) Transcript profiles in longissimus dorsi muscle and subcutaneous adipose tissue: A comparison of pigs with different postweaning growth rates. *Journal of Animal Science* **93**, 2134–2143.

Pillman K.A., Scheer K.G., Hackett-Jones E., Saunders K., Bert A.G., Toubia J. *et al.* (2019) Extensive transcriptional responses are co-ordinated by microRNAs as revealed by Exon–Intron Split Analysis (EISA). *Nucleic Acids Research* **47**, 8606-8619.

Puig-Oliveras A., Ramayo-Caldas Y., Corominas J., Estellé J., Pérez-Montarelo D., Hudson N.J. *et al.* (2014) Differences in muscle transcriptome among pigs phenotypically extreme for fatty acid composition. *PLoS One* **9**, e99720.

Reverter A. & Chan E.K.F. (2008) Combining partial correlation and an information theory approach to the reversed engineering of gene co-expression networks. *Bioinformatics* **24**, 2491–2497.

Robinson M.D. & Oshlack A. (2010) A scaling normalization method for differential

1021 expression analysis of RNA-seq data. *Genome Biology* **11**, R25.

1022 Robinson M.D., McCarthy D.J. & Smyth G.K. (2010) edgeR: a Bioconductor package
1023 for differential expression analysis of digital gene expression data.
1024 *Bioinformatics* **26**, 139–40.

1025 Schaefke B., Sun W., Li Y.-S., Feng L. & Chen W. (2018) The evolution of
1026 posttranscriptional regulation. *Wiley Interdisciplinary Reviews* **9**, e1485.

1027 Tamahara T., Ochiai K., Muto A., Kato Y., Sax N., Matsumoto M. *et al.* (2017) The
1028 mTOR-Bach2 cascade controls cell cycle and class switch recombination during
1029 B cell differentiation. Molecular and Cellular Biology **37**, e00418-17.

1030 Tao R., Xiong X., Liangpunsakul S. & Dong X.C. (2015) Sestrin 3 protein enhances
1031 hepatic insulin sensitivity by direct activation of the mTORC2-Akt signaling.
1032 *Diabetes* **64**, 1211–1223.

1033 Tarbier M., Mackowiak S.D., Frade J., Catuara-Solarz S., Biryukova I., Gelali E. *et al.*
1034 (2020) Nuclear gene proximity and protein interactions shape transcript
1035 covariations in mammalian single cells. *Nature Communications* **11**, 5445.

1036 Ussar S., Bezy O., Blüher M. & Kahn C.R. (2012) Glypican-4 enhances insulin
1037 signaling via interaction with the insulin receptor and serves as a novel
1038 adipokine. *Diabetes* **61**, 2289–2298.

1039 Velázquez-Cruz A., Baños-Jaime B., Díaz-Quintana A., la Rosa M.A.D. & Díaz-
1040 Moreno I. (2021) Post-translational control of RNA-binding proteins and disease-
1041 related dysregulation. *Frontiers in Molecular Biosciences* **8**, 658852.

1042 Wang Y., Yan S., Xiao B., Zuo S., Zhang Q., Chen G. *et al.* (2018) Prostaglandin F 2α
1043 facilitates hepatic glucose production through CaMKIIγ/p38/FOXO1 signaling
1044 pathway in fasting and obesity. *Diabetes* **67**, 1748–1760.

1045 Warr A., Affara N., Aken B., Beiki H., Bickhart D.M., Billis K. *et al.* (2020) An

improved pig reference genome sequence to enable pig genetics and genomics research. *Gigascience* **9**, 1–14.

Watson-Haigh N.S., Kadarmideen H.N. & Reverter A. (2010) PCIT: an R package for weighted gene co-expression networks based on partial correlation and information theory approaches. *Bioinformatics* **26**, 411–413.

Wei W., Li B., Liu K., Jiang A., Dong C., Jia C. *et al.* (2018) Identification of key microRNAs affecting drip loss in porcine longissimus dorsi by RNA-seq. *Gene* **64**, 276–282.

Wu D., Hu D., Chen H., Shi G., Fetahu I.S., Wu F. *et al.* (2018) Glucose-regulated phosphorylation of TET2 by AMPK reveals a pathway linking diabetes to cancer. *Nature* **559**, 637–641.

Xiao B., Gu S.M., Li M.J., Li J., Tao B., Wang Y. *et al.* (2015) Rare SNP rs12731181 in the miR-590-3p target site of the Prostaglandin F2α receptor gene confers risk for essential hypertension in the Han Chinese population. *Arteriosclerosis, Thrombosis and Vascular Biology* **35**, 1687–1695.

Xie S., Li X., Qian L., Cai C., Xiao G., Jiang S. *et al.* (2019) An integrated analysis of mRNA and miRNA in skeletal muscle from myostatin-edited Meishan pigs. *Genome* **62**, 305–315.

Xu J., Bao X., Peng Z., Wang L., Du L. & Niu W. (2016) Comprehensive analysis of genome-wide DNA methylation across human polycystic ovary syndrome ovary granulosa cell. *Oncotarget* **7**, 27899-27909.

Xu S., Ni H., Chen H. & Dai Q. (2019) The interaction between STAT3 and nAChRα1 interferes with nicotine-induced atherosclerosis via Akt/mTOR signaling cascade. *Aging* **11**, 8120–8138.

Yang J. & Shi B. yin (2021) Dickkopf (Dkk)-2 is a beige fat-enriched adipokine to

regulate adipogenesis. *Biochemical and Biophysical Research Communications* **548**, 211–216.

Yang W., Kelly T. & He J. (2007) Genetic epidemiology of obesity. *Epidemiologic Reviews* **29**, 49–61.

Yeung F., Ramírez C.M., Mateos-Gomez P.A., Pinzaro A., Ceccarini G., Kabir S. *et al.* (2013) Nontelomeric role for Rap1 in regulating metabolism and protecting against obesity. *Cell Reports* **3**, 1847–1856.

Zhang C., Zhang B., Zhang X., Sun G. & Sun X. (2020) Targeting orphan nuclear receptors NR4As for energy homeostasis and diabetes. *Frontiers in Pharmacology* **11**, 587457.

Zhang L., Chen Z., Wang Y., Tweardy D.J. & Mitch W.E. (2020) Stat3 activation induces insulin resistance via a muscle-specific E3 ubiquitin ligase Fbxo40. *American Journal of Physiology, Endocrinology and Metabolism* **318**, E625–E635.

Zhang S., Hulver M.W., McMillan R.P., Cline M.A. & Gilbert E.R. (2014) The pivotal role of pyruvate dehydrogenase kinases in metabolic flexibility. *Nutrition & Metabolism* **11**, 10.

Zhao B.S., Roundtree I.A. & He C. (2017) Post-transcriptional gene regulation by mRNA modifications. *Nature Reviews Molecular Cell Biology* **18**, 31-42.

Zhou Y. & Rui L. (2013) Leptin signaling and leptin resistance. *Frontiers of Medicine* **7**, 207–222.

Table 1: mRNA genes with the top 5% post-transcriptional (PTc) scores and at least 2-fold exonic fraction (ΔEx) reduction (equivalent to -1 in the $\log_2$ scale) of *gluteus medius* skeletal muscle samples from fasting (*AL-T0*, N = 11) and fed (*AL-T2*, N = 12) Duroc gilts.

ID	Gene	$\log_2$FC[a]	ΔEx[b]	PTc[c]	*P*-value	*q*-value	DE[d]	miRNA target
ENSSSCG00000032094	*DKK2*	-2.010	-1.431	-4.738	1.654E-05	3.830E-03		x
ENSSSCG00000015334	*PDK4*	-2.108	-5.250	-4.698	4.693E-03	1.330E-01	x	x
ENSSSCG00000015037	*IL18*	-1.655	-1.191	-3.682	4.787E-03	1.340E-01	x	x
ENSSSCG00000005385	*NR4A3*	-1.337	-3.082	-3.646	4.038E-02	4.098E-01	x	x
ENSSSCG00000003766	*DNAJB4*	-1.391	-1.008	-3.348	8.358E-03	1.905E-01		x
ENSSSCG00000015969	*CHRNA1*	-1.561	-1.339	-3.341	2.606E-03	9.406E-02	x	x
ENSSSCG00000039419	*SLCO4A1*	-1.055	-2.279	-3.180	2.820E-02	3.544E-01	x	x
ENSSSCG00000049158		-1.107	-1.096	-3.164	3.182E-02	3.735E-01		x
ENSSSCG00000004347	*FBXL4*	-1.298	-1.126	-3.133	1.422E-03	6.520E-02	x	x
ENSSSCG00000004979	*MYO9A*	-1.239	-1.003	-3.043	7.296E-03	1.731E-01		x
ENSSSCG00000013351	*NAV2*	-1.163	-1.196	-2.863	2.605E-04	2.301E-02	x	x
ENSSSCG00000032741	*TBC1D9*	-0.913	-1.061	-2.736	1.534E-02	2.583E-01		x
ENSSSCG00000031728	*ABRA*	-1.238	-1.393	-2.704	1.295E-03	6.116E-02	x	x
ENSSSCG00000006331	*PBX1*	-0.891	-1.039	-2.480	1.135E-02	2.177E-01	x	x
ENSSSCG00000035037	*SIK1*	-1.357	-1.289	-2.475	3.999E-03	1.212E-01	x	x
ENSSSCG00000038374	*CIART*	-1.027	-1.321	-2.052	1.543E-02	2.587E-01	x	
ENSSSCG00000023806	*LRRN1*	-0.776	-1.013	-1.983	1.580E-01	7.074E-01		x
ENSSSCG00000009157	*TET2*	-0.381	-1.123	-1.792	4.880E-01	9.582E-01		x
ENSSSCG00000011133	*PFKFB3*	-0.022	-2.256	-1.785	9.712E-01	9.987E-01	x	x
ENSSSCG00000002283	*FUT8*	-0.578	-1.286	-1.784	9.887E-02	6.059E-01	x	x
ENSSSCG00000023133	*OSBPL6*	-0.432	-1.088	-1.772	3.835E-01	9.108E-01	x	
ENSSSCG00000017986	*NDEL1*	-0.767	-1.644	-1.759	1.006E-02	2.081E-01	x	x
ENSSSCG00000031321	*NR4A1*	-0.630	-1.328	-1.720	6.298E-02	5.006E-01	x	
ENSSSCG00000035101	*KLF5*	-0.519	-1.487	-1.708	2.942E-01	8.488E-01	x	x
ENSSSCG00000004332	*BACH2*	-0.714	-2.105	-1.705	9.089E-02	5.861E-01	x	x
ENSSSCG00000017983	*PER1*	-0.773	-1.073	-1.627	3.000E-02	3.662E-01	x	

[a]$\log_2$FC: estimated $\log_2$ fold change for mean exonic fractions from *gluteus medius* skeletal muscle samples of fasted *AL-T0* and fed *AL-T2* Duroc gilts; [b]ΔEx: exonic fraction increment ($Ex_2 - Ex_1$) in $\log_2$ scale when comparing exon abundances in *AL-T0* (Ex_1) vs *AL-T2* (Ex_2) Duroc gilts; [c]PTc: post-transcriptional signal (ΔEx – ΔInt) in z-score scale. The *q*-value has been calculated with the false discovery rate (FDR) approach (Benjamini & Hochberg 1995). [d]DE: The "x" symbols indicate differentially expressed (DE) and downregulated genes (FC < -2; *q*-value < 0.05) according to their exonic counts, as well as those mRNA genes targeted by at least one of the upregulated miRNAs excluding redundant seeds (N = 6, **Table S5**).

Table 2: mRNA genes with the top 5% post-transcriptional (PTc) scores and at least 2-fold exonic fraction (ΔEx) reduction (equivalent to -1 in the log2 scale) of adipocytes from *lean* (N = 5) and *obese* (N = 5) Duroc-Göttingen minipigs classified in accordance with their body mass index.

mRNA	Gene	log_2FC[a]	ΔEx[b]	PTc[c]	*P*-value	*q*-value	DE[d]	miRNA target
ENSSSCG00000010814	*ESRRG*	-0.591	-5.305	-6.425	7.364E-01	9.996E-01		x
ENSSSCG00000037015	*SESN3*	-2.000	-1.378	-5.707	2.541E-07	2.477E-03	x	x
ENSSSCG00000032452	*WFS1*	-2.198	-2.138	-5.510	9.509E-03	9.996E-01	x	
ENSSSCG00000039548	*PTGFR*	-1.634	-1.590	-4.915	8.804E-03	9.996E-01		x
ENSSSCG00000013829	*SYDE1*	-1.670	-1.160	-4.188	5.795E-04	6.000E-01	x	
ENSSSCG00000002265	*FAM174B*	-1.244	-1.726	-4.179	5.385E-02	9.996E-01		x
ENSSSCG00000016233	*SERPINE2*	-1.735	-2.060	-3.603	5.684E-02	9.996E-01	x	x
ENSSSCG00000006243	*PENK*	-0.420	-2.104	-3.573	7.628E-01	9.996E-01		
ENSSSCG00000038879	*RELB*	-1.272	-1.056	-3.512	3.659E-03	9.996E-01	x	
ENSSSCG00000023408	*SAMD4A*	-1.328	-1.156	-3.509	4.486E-02	9.996E-01		x
ENSSSCG00000008449	*SLC3A1*	-1.014	-1.154	-3.491	5.859E-02	9.996E-01		
ENSSSCG00000014921	*PRSS23*	-1.141	-1.739	-3.360	2.719E-01	9.996E-01		x
ENSSSCG00000017186	*RNF157*	-1.218	-2.338	-3.317	2.413E-01	9.996E-01	x	x
ENSSSCG00000035403	*RFX2*	-1.109	-1.022	-2.958	1.550E-01	9.996E-01		x
ENSSSCG00000010893		-0.655	-1.352	-2.931	4.068E-01	9.996E-01		x
ENSSSCG00000031819	*TP53I11*	-1.002	-1.711	-2.883	4.102E-01	9.996E-01		x
ENSSSCG00000017137	*METRNL*	-0.674	-1.102	-2.812	2.422E-01	9.996E-01		
ENSSSCG00000032562	*TMC6*	-0.837	-1.152	-2.765	2.078E-01	9.996E-01		
ENSSSCG00000031261	*RHOQ*	-0.903	-1.046	-2.750	1.839E-02	9.996E-01	x	
ENSSSCG00000001089	*GPLD1*	-0.872	-1.761	-2.723	4.302E-01	9.996E-01		x
ENSSSCG00000034259	*PMEPA1*	-0.880	-1.348	-2.720	3.583E-01	9.996E-01		x
ENSSSCG00000017014	*PANK3*	-0.614	-1.037	-2.557	2.288E-01	9.996E-01		x
ENSSSCG00000003377	*ACOT7*	-0.790	-2.688	-2.544	3.439E-01	9.996E-01	x	
ENSSSCG00000010079	*PPM1F*	-0.762	-1.035	-2.473	4.967E-02	9.996E-01	x	x
ENSSSCG00000040464	*LEP*	-0.747	-2.186	-2.463	1.880E-01	9.996E-01	x	x
ENSSSCG00000022029	*RAP1GAP*	-0.120	-1.109	-2.418	8.822E-01	9.996E-01		x
ENSSSCG00000022099	*TP53INP2*	-0.628	-1.058	-2.403	3.683E-01	9.996E-01		
ENSSSCG00000025652	*CDH1*	-0.472	-2.592	-2.372	6.533E-01	9.996E-01		x
ENSSSCG00000027266	*PNPLA3*	-0.443	-1.386	-2.198	5.725E-01	9.996E-01		
ENSSSCG00000015401	*PCLO*	-0.674	-1.492	-2.182	4.537E-01	9.996E-01		x
ENSSSCG00000020872		-1.029	-1.128	-2.090	1.340E-01	9.996E-01		
ENSSSCG00000032633	*FAM53A*	-0.749	-1.033	-2.066	4.576E-02	9.996E-01	x	
ENSSSCG00000015559	*NCF2*	-0.679	-1.221	-2.061	3.570E-01	9.996E-01		x
ENSSSCG00000015766	*WDR17*	-0.609	-1.139	-1.998	2.093E-01	9.996E-01		
ENSSSCG00000009761	*NCOR2*	-0.681	-1.421	-1.913	2.643E-01	9.996E-01		
ENSSSCG00000016928	*RAB3D*	-0.491	-1.142	-1.888	2.953E-01	9.996E-01		
ENSSSCG00000011230	*OSBPL10*	-0.576	-1.594	-1.869	4.272E-01	9.996E-01		x
ENSSSCG00000017298	*TANC2*	-0.615	-1.541	-1.846	4.896E-01	9.996E-01		
ENSSSCG00000007899		-0.524	-1.036	-1.814	4.500E-01	9.996E-01		x

ENSSSCG00000026421	*PKD2L2*	-0.463	-1.230	-1.800	5.098E-01	9.996E-01		
ENSSSCG00000015332	*PON1*	-0.626	-1.076	-1.763	2.530E-01	9.996E-01	x	x
ENSSSCG00000009215	*ABCG2*	-0.455	-1.446	-1.749	5.684E-01	9.996E-01		
ENSSSCG00000017328	*ARHGAP27*	-0.235	-2.788	-1.699	8.113E-01	9.996E-01	x	x
ENSSSCG00000017199	*TRIM47*	-0.362	-1.057	-1.645	6.717E-01	9.996E-01		x

[a]Log_2FC: estimated log_2 fold change for mean exonic fractions from adipocytes of *lean* and *obese* Duroc-Göttingen minipigs.; [b]ΔEx: exonic fraction increment ($Ex_2 – Ex_1$) in log_2 scale when comparing exon abundances in obese (Ex_1) vs lean (Ex_2) Duroc-Göttingen minipigs; [c]PTc: post-transcriptional signal (ΔEx – ΔInt) in z-score scale. The *q*-value has been calculated with the false discovery rate (FDR) approach (Benjamini & Hochberg 1995). [d]DE: The "x" symbols indicate differentially expressed (DE) and downregulated genes (FC < -2; *q*-value < 0.05) according to their exonic counts, as well as those mRNA genes targeted by at least one of the upregulated miRNAs excluding redundant seeds (N = 4, **Table S10**).

Figures

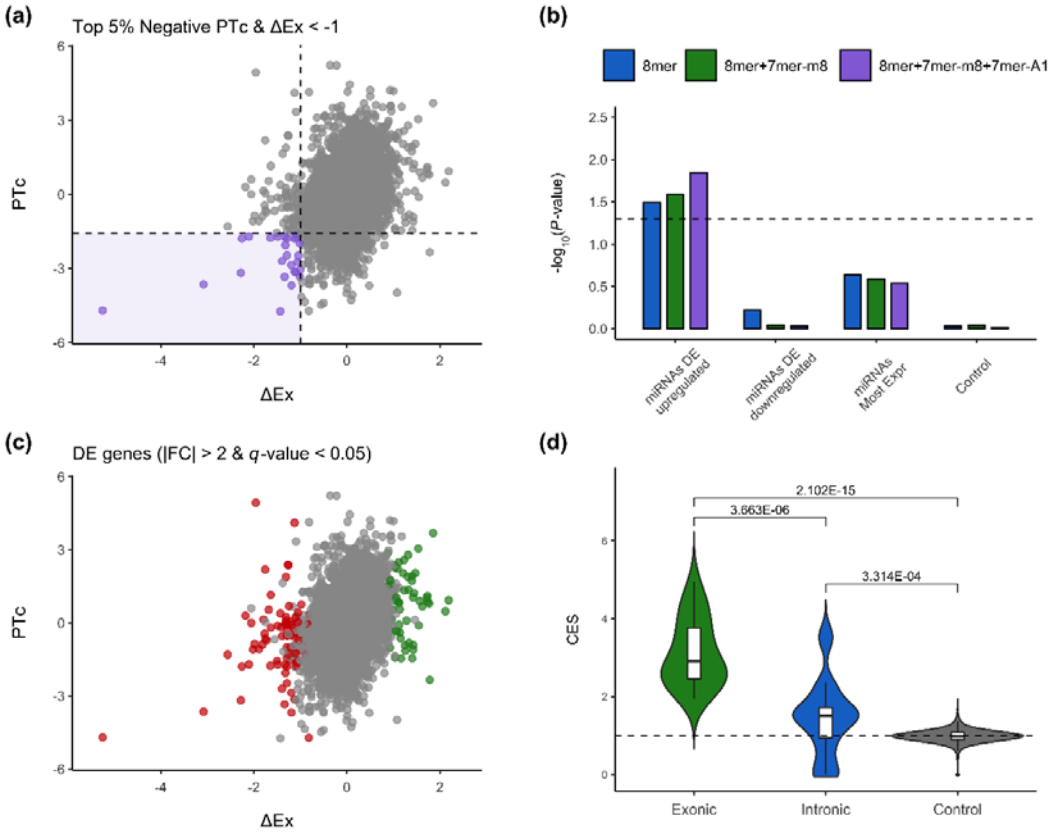

Figure 1: (**a**) Scatterplot depicting mRNA genes with the top 5% negative PTc scores and at least 2-fold ΔEx reduction (equivalent to -1 in the $\log_2$ scale) according to their exonic (ΔEx) and PTc (ΔEx – ΔInt) values (in purple and delimited by dashed lines) and putatively targeted by DE upregulated miRNAs (FC > 1.5; *q*-value < 0.05) expressed in the *gluteus medius* skeletal muscle of fasted (*AL-T0*, N = 11) and fed (*AL-T2*, N = 12) Duroc gilts. (**b**) Enrichment analyses of the set of mRNA genes with the top 5% negative PTc scores and at least 2-fold ΔEx reduction putatively targeted by DE upregulated miRNAs (FC > 1.5; *q*-value < 0.05), DE downregulated miRNAs (FC < -1.5; *q*-value < 0.05) and the top 5% most highly expressed miRNAs, excluding DE

upregulated miRNAs. As indicated with the dashed line, a nominal *P*-value = 0.05 was set as a significance threshold. (**c**) Scatterplot depicting DE upregulated (in green) and downregulated (in red) genes (|FC| > 2; *q*-value < 0.05) according to their exonic (ΔEx) and PTc (ΔEx – ΔInt) values. (**d**) Covariation enrichment scores (CES) for the exonic and intronic fractions of mRNA genes (N = 21) with the top 5% negative PTc scores and at least 2-fold ΔEx reduction that were putatively targeted by upregulated miRNAs (N = 6) in the *gluteus medius* skeletal muscle of fasted (*AL-T0*, N = 11) and fed (*AL-T2*, N = 12) Duroc gilts. The control set was defined by generating random permuted lists (N = 1,000) of 21 genes and using their exonic and intronic fractions for calculating their CES values. Statistical significance was assessed using a Mann-Whitney U non-parametric test (Mann & Whitney 1947). The dashed line represents a CES of 1, equivalent to an observed null fold change in covariation.

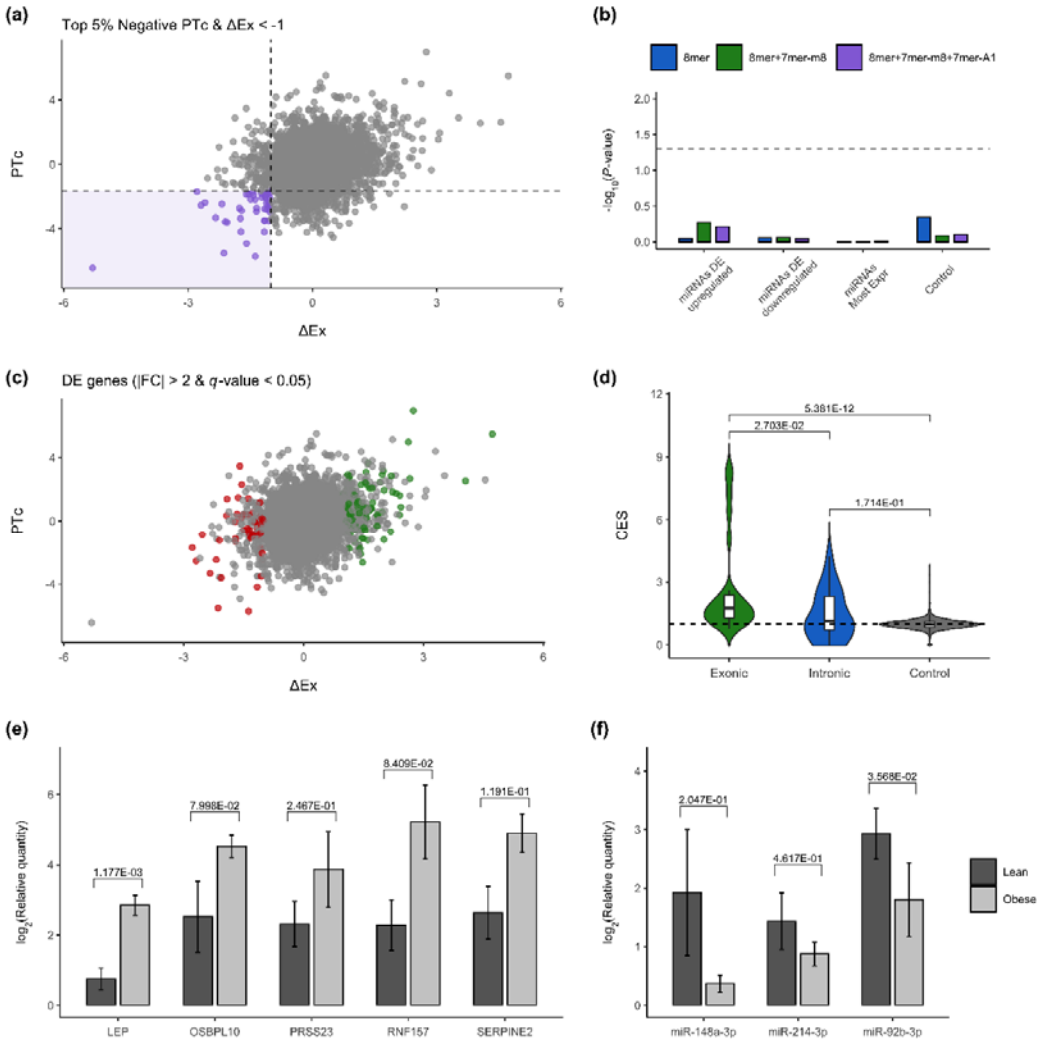

Figure 2: (a) Scatterplot depicting mRNA genes with the top 5% negative PTc scores and at least 2-fold ΔEx reduction (equivalent to -1 in the $\log_2$ scale) according to their exonic (ΔEx) and PTc (ΔEx – ΔInt) values (in purple and delimited by dashed lines) and putatively targeted by upregulated miRNAs (FC > 1.5; *P*-value < 0.01) from fat samples obtained from Duroc-Göttingen minipigs with *lean* (N = 5) and *obese* (N = 5) phenotypes classified according to their body mass index (BMI). **(b)** Enrichment analyses of the number of mRNA genes with the top 5% negative PTc scores and at least 2-fold ΔEx reduction putatively targeted by DE upregulated miRNAs (FC > 1.5; *q*-

value < 0.05), DE downregulated miRNAs (FC < -1.5; *q*-value < 0.05) and the top 5% most highly expressed miRNAs, excluding DE upregulated miRNAs. As indicated with the dashed line, a nominal *P*-value = 0.05 was set as a significance threshold. **(c)** Scatterplot depicting DE upregulated (in green) and downregulated (in red) genes (|FC| > 2; *q*-value < 0.05) according to their exonic (ΔEx) and PTc (ΔEx – ΔInt) values. **(d)** Covariation enrichment scores (CES) for the exonic and intronic fractions of mRNA genes (N = 25) with the top 5% negative PTc scores and at least 2-fold ΔEx reduction that were putatively targeted by upregulated miRNAs (N = 4) from fat samples obtained from Duroc-Göttingen minipigs with *lean* (N = 5) and *obese* (N = 5) phenotypes. The control set was defined by generating random permuted lists (N = 1,000) of 25 genes and using their exonic and intronic fractions for calculating their CES values. Statistical significance was assessed using a Mann-Whitney U non-parametric test (Mann & Whitney 1947). The dashed line represents a CES of 1, equivalent to an observed null fold change in covariation. **(e)** Barplots depicting qPCR $\log_2$ transformed relative quantities (Rq) for *LEP*, *OSBPL10*, *PRSS23*, *RNF157* and *SERPINE2* mRNA transcripts measured in adipocytes from the retroperitoneal fat of *lean* (N = 5) and *obese* (N = 5) Duroc-Göttingen minipigs. **(f)** Barplots depicting qPCR $\log_2$ transformed relative quantities (Rq) for ssc-miR-148a-3p, ssc-miR-214-3p and ssc-miR-92b-3p miRNA transcripts measured in the isolated adipocytes from the retroperitoneal fat of *lean* (N = 5) and *obese* (N = 5) Duroc-Göttingen minipigs.

Supplementary Tables

Table S1: Phenotypic values for 11 Duroc-Göttingen minipigs from the F2-UNIK resource population classified as *obese* or *lean* in accordance with their body mass index.

Table S2: Primers for qPCR validation of selected mRNAs (among those with the top 5% negative PTc scores and at least 2-fold ΔEx reduction) and miRNAs (DE upregulated) in the F2-UNIK Duroc-Göttingen minipig population after comparing *lean* (N = 5) and *obese* (N = 5) individuals.

Table S3: Raw Cq values obtained in qPCR analyses measuring adipocyte expression levels of selected mRNAs and miRNAs from *lean* (N = 5) and *obese* (N = 5) Duroc-Göttingen minipigs.

Table S4: Genes detected by the *edgeR* tool as differentially expressed when comparing *gluteus medius* expression profiles of fasted *AL-T0* (N = 11) and fed *AL-T2* (N = 12) Duroc gilts.

Table S5: microRNAs detected by the *edgeR* tool as differentially expressed when comparing *gluteus medius* expression profiles of fasted *AL-T0* (N = 11) and fed *AL-T2* (N = 12) Duroc gilts.

Table S6: Post-transcriptional (PTc) and transcriptional (Tc) signals detected with EISA in genes expressed in *gluteus medius* skeletal muscle samples from fasted (*AL-T0*, N = 11) and fed (*AL-T2*, N = 12) Duroc gilts.

Table S7: Binding sites of DE upregulated miRNAs (N = 6) found in the 3'-UTRs of mRNA genes with the top 5% negative PTc scores and at least 2-fold reduction in the exonic fraction (ΔEx) of *gluteus medius* skeletal muscle samples from fasting (*AL-T0*, N = 11) and fed (*AL-T2*, N = 12) Duroc gilts.

Table S8: Covariation enrichment scores (CES) for the exonic and intronic fractions of mRNA genes with the top 5% negative post-transcriptional signals (PTc) and at least 2-fold reduction in their exonic (ΔEx) fraction predicted to be targeted by DE upregulated miRNAs (N = 6) of *gluteus medius* skeletal muscle expression profiles from fasting (*AL-T0*, N = 11) and fed (*AL-T2*, N = 12) Duroc gilts.

Table S9: Genes detected by the *edgeR* tool as differentially expressed when comparing adipocyte expression profiles from *lean* (N = 5) and *obese* (N = 5) Duroc-Göttingen minipigs classified in accordance with their body mass index.

Table S10: microRNA genes detected by the *edgeR* tool as differentially expressed when comparing adipocyte expression profiles from *lean* (N = 5) and *obese* (N = 5) Duroc-Göttingen minipigs classified in accordance with their body mass index.

Table S11: Post-transcriptional (PTc) and transcriptional (Tc) signals detected with EISA in genes expressed in adipocytes from *lean* (N = 5) and *obese* (N = 5) Duroc-Göttingen minipigs classified in accordance with their body mass index.

Table S12: Binding sites of DE upregulated miRNAs (N = 4) found in the 3'-UTRs of mRNA genes with the top 5% negative PTc scores and at least 2-fold reduction in the exonic fraction (ΔEx) of adipocyte from *lean* (N = 5) and *obese* (N = 5) Duroc-Göttingen minipigs classified in accordance with their body mass index.

Table S13: Covariation enrichment scores (CES) for the exonic and intronic fractions of mRNA genes with the top 5% negative post-transcriptional signals (PTc) and at least 2-fold reduction in their exonic (ΔEx) fraction predicted to be targeted by DE upregulated miRNAs (N = 4) of adipocyte expression profiles from *lean* (N = 5) and *obese* (N = 5) Duroc-Göttingen minipigs classified in accordance with their body mass index.